Atmos. Chem. Phys., 13, 11573–11594, 2013
www.atmos-chem-phys.net/13/11573/2013/
doi:10.5194/acp-13-11573-2013

Atmospheric Chemistry and Physics Open Access

Long-term observations of cluster ion concentration, sources and sinks in clear sky conditions at the high-altitude site of the Puy de Dôme, France

C. Rose[1], J. Boulon[1], M. Hervo[1], H. Holmgren[1], E. Asmi[2], M. Ramonet[3], P. Laj[4], and K. Sellegri[1]

[1]Laboratoire de Météorologie Physique CNRS UMR6016, Observatoire de Physique du Globe de Clermont-Ferrand, Université Blaise Pascal, France
[2]Finnish Meteorological Institute, P.O. Box 503, 00101 Helsinki, Finland
[3]Laboratoire des Sciences du Climat et de l'Environnement, UMR Commissariat à l'Energie Atomique/CNRS 1592, Gif-sur-Yvette, France
[4]Laboratoire de Glaciologie et Géophysique de l'Environnement, CNRS UMR5183, Université Joseph Fourier Grenoble 1, Saint Martin d'Héres, France

Correspondence to: C. Rose (c.rose@opgc.univ-bpclermont.fr)

Received: 14 May 2013 – Published in Atmos. Chem. Phys. Discuss.: 5 June 2013
Revised: 27 October 2013 – Accepted: 29 October 2013 – Published: 28 November 2013

Abstract. Cluster particles (0.8–1.9 nm) are key entities involved in nucleation and new particle formation processes in the atmosphere. Cluster ions were characterized in clear sky conditions at the Puy de Dôme station (1465 m a.s.l.). The studied data set spread over five years (February 2007–February 2012), which provided a unique chance to observe seasonal variations of cluster ion properties at high altitude. Statistical values of the cluster ion concentrations and diameters are reported for both positive and negative polarities. Cluster ions were found to be ubiquitous at the Puy de Dôme and displayed an annual variation with lower concentrations in spring. Positive cluster ions were less numerous than negative, but were larger in diameter. Negative cluster ion properties were not sensitive to the occurrence of a new particle formation (NPF) event, while positive cluster ions appeared to be significantly more numerous and larger on event days. The parameters of the balance equation for the positive cluster concentration are reported separately for the different seasons and for the NPF event days and non-event days. The steady-state assumption suggests that the ionization rate is balanced with two sinks: the ion recombination and the attachment onto background aerosol particles, referred to as "aerosol ion sink". The aerosol ion sink was predominant compared to the recombination sink. The positive ionization rates derived from the balance equation (Q_{calc}) were well correlated with the ionization rates obtained from radon measurement (Q_{meas}). When ignoring the gamma radiation contribution to the ion production, Q_{calc} is on average higher than Q_{meas} during the warm season. In contrast, when a seasonal gamma contribution is taken into account, Q_{meas} always exceeds Q_{calc}. We found that neither the aerosol ion sink nor the ionization rate (calculated or measured, with or without the gamma contribution) were significantly different on event days compared to non-event days, and thus, they were not able to explain the different positive cluster concentrations between event and non-event days. Hence, the excess of positive small ions on event days may derive from an additional constant source of ions leading to a non-steady state.

1 Introduction

In polluted areas, atmospheric aerosol particles often affect visibility and have undesirable effects on human health (Seaton et al., 1995). On a more global scale, aerosol particles influence the Earth's climate system by scattering and absorbing incoming solar radiation (direct effect) and by affecting several cloud properties (indirect effect). Despite the fact that atmospheric research, especially climate and pollution studies, has been the focus of the scientific community

during recent decades, the radiative forcing associated to the aerosol indirect effect still has a large uncertainty (IPCC, 2007).

A better understanding of the indirect effect requires, in particular, more accurate information on secondary aerosol particle sources and thus on the nucleation process. Measurements, as well as recent model investigations, suggest that atmospheric nucleation is an important source of aerosol particles and cloud condensation nuclei (CCN) (Kerminen et al., 2012; Makkonen et al., 2012) but the very first steps of the nucleation process remain uncertain. Indeed, the formation and growth of ultrafine aerosol particles in the atmosphere has been studied during recent decades in various locations (see Kulmala et al., 2004 for a review) but the mechanisms involved in the particle formation are still unclear, mostly because of instrumental limitations.

Much effort has been made during the last few years to develop instruments able to detect freshly nucleated neutral particles down to 1 nm sizes. Since electrical methods used in the NAIS (Neutral cluster and Air Ion Spectrometer; Mirme and Mirme, 2013) cannot ensure reliable concentrations for neutral particles smaller than ∼1.6–1.7 nm due to the post-filtering process of corona-generated ions (Asmi et al., 2009; Manninen et al., 2011), condensation particle-counting methods have been more deeply investigated, especially with the Particle Size Magnifier (PSM) (see for example Kim et al., 2003; Vanhanen et al., 2011; Kuang et al., 2012). However, in their recent paper, Kangasluoma et al. (2013) have shown that in the case of the PSM, measurements were greatly dependent on both the relative humidity and the chemical composition of the sampled particles. In that case, data analysis requires a very good knowledge of the sampling conditions and calibrations corresponding to the prevailing conditions. That is why the study of air ions certainly remains a robust path to gain information on the smallest cluster particles (here particles with mobilities up to 3.162 $cm^2\ V^{-1}\ s^{-1}$ in NTP conditions, corresponding to a mobility diameter, i.e. Millikan diameter, of 0.8 nm; see Mäkelä et al. (1996) for more details on the law of size – mobility conversion applied in this work).

Air ions are carriers of electrical current in the atmosphere. The air ion population is commonly divided into small, or cluster, intermediate and large ions. The "cluster ions" or "small ions", which are in the scope of this paper, are the ions with a mobility diameter greater than 0.5 $cm^2\ V^{-1}\ s^{-1}$ (roughly corresponding to particle Millikan diameters smaller than 1.9 nm). Thus, they are the most relevant for new particle formation studies, which explains why their behaviour has already been deeply studied in various locations. A recent review article by Hirsikko et al. (2011) based on ca. 260 publications provides an overview of the main observations concerning small ions concentration as well as their connection with nucleation. Atmospheric cluster ions are produced by external radiation, such as gamma radiation and galactic cosmic rays (GCR), and by airborne radionuclides, mainly radon and thoron. Above the ocean, GCR are the principal source for cluster ions (Hensen and Van der Hage, 1994) while in continental areas, the production of ions is mostly due to external radiation. External radiation displays seasonal variations while daily variation of the small ion production is mainly driven by the variation of the radon and thoron concentrations (Laakso et al., 2004; Hirsikko et al., 2007b).

The ionization rates have been well studied during the last century and overviews of the earliest results can be found in Chalmers (1967) and Israël (1970). The ionization rate strongly depends on the measurement site since it is affected by different factors such as the content of radioactive matter in the ground, the soil properties, the snow cover and the orography. In addition, the altitude was shown to have an influence on the ionization rate (Rosen et al., 1985). Tammet et al. (2006) reported measurements performed at two different heights in Hyytiälä, Finland, (2 and 14 m). They observed higher cluster concentrations at 2 m, which could be explained by a reduced vegetal sink and increased ion production by radon activity close to the ground. The role of radon was also pointed out by Dhanorkar and Kamra (1994) in Pune, India, where the highest cluster concentrations coincided with weak mixing and incoming air enriched with radon from the surrounding mountains.

Ions are believed to be involved in nucleation processes, through the ion induced nucleation mechanism (Laakso et al., 2002; Lovejoy et al., 2004; Luts et al., 2006; Kazil et al., 2008; Nieminen et al., 2011). A connection between GCR, aerosols and clouds through the nucleation process was proposed by Dickinson (1975): sulphate aerosol particles forming from ions produced by GCR might grow to CCN sizes and form cloud droplets. In that case, the variation of GCR ionization over the solar cycle would have a direct impact on cloud properties (lifetime, albedo) and thus on the radiative forcing of the Earth. However, more recent studies did not find significant support for a correlation between the variation in GCR ionization and low cloud cover (Sloan and Wolfendale, 2008). For the ion-induced nucleation mechanism, the ionization rate is a key entity governing the nucleation rate.

The ionization rate can be obtained from direct measurements or it can be derived from calculations based on the balance equation for the concentration of small ions (Israël, 1970). Small ion properties including ionization rate have been discussed in various environments (Hõrrak et al., 2003, 2008; Vana et al., 2008; Yli-Juuti et al., 2009). For example, the small ion population was shown to be very sensitive to the presence of clouds at high-altitude sites (Lihavainen et al., 2007; Venzac et al., 2007). The authors have reported that in cloudy conditions small ions were mainly lost on cloud droplets while in clear sky conditions aerosol particles and the ion-ion recombination process were responsible for the loss of ions. All the studies previously mentioned are based on data sets rarely exceeding one year. To our knowledge, the

analysis proposed in this paper is the first one based on such an extended data set for small ion properties.

We report seasonal and diurnal variability of cluster ion concentration and size measured over a five-year period (February 2007–February 2012) in clear sky conditions at the Puy de Dôme station (corresponding to 842 days). Cluster ions were measured with an Air Ion Spectrometer (AIS) which detects ions in the range of 0.0013–3.2 $cm^2\ V^{-1}\ s^{-1}$, corresponding to particle diameters between 0.8 and 42 nm. The behaviour of positive cluster ions is specifically investigated, with the goal of identifying the sinks and sources responsible for the reported positive cluster ion concentrations, with a special focus on the differences observed between new particle formation event days and non-event days.

2 Measurements and methods

2.1 Measurement site

Measurements were conducted at the Puy de Dôme (PDD) site in central France (45°46′ N, 2°57′ E) which is part of the EMEP/GAW/ACTRIS networks. The station is located at the top of the Puy de Dôme mountain (1465 m a.s.l.), which is one of the youngest volcanoes of the Chaine des Puys. It is also the highest, with a height of 550 m relative to its base. The station is situated in an environment mainly characterized by fields and forest but one should note the presence of a TV transmitter antenna (73 m high) close to the station, at the top of the mountain. The nearest city, Clermont-Ferrand (300 000 inhabitants), is located 16 km east of the mountain. A more complete description of the station can be found in Asmi et al. (2011) and Freney et al. (2011).

2.2 The Air Ion Spectrometer (AIS)

The ion size distributions were measured with (N)AIS (Airel Ltd., Mirme et al., 2007, Mirme and Mirme, 2013) which allows ion detection in the mobility range 0.0013–3.2 $cm^2\ V^{-1}\ s^{-1}$, corresponding to mobility diameter, i.e. Millikan diameter, of 0.8–42 nm (Mäkelä et al., 1996). During the whole measurement period, three different instruments were used, the AIS 7, NAIS 3 and NAIS 13. From February 2007 to the end of 2010, the instrument was operating in a shelter, with a short inlet (length 30 cm, inner diameter 3 cm), sampling approximately 2 m high from the ground. At the end of 2010, the instrument moved onto the roof of a station located close to the temporary shelter, sampling 11 m high from the ground with the same individual non-heated short inlet. For the two different measurement setups, one should note that measured ion size distributions were directly influenced by the presence of a cloud.

The AIS has two identical, cylindrical Differential Mobility Analyzers (DMA) for the simultaneous measurement of positive and negative ions. Each analyser has a sample flow rate of 30 L min^{-1} and a sheath flow rate of 60 L min^{-1}. Such high flow rates are used to avoid diffusion losses and ensure a significant signal to noise ratio, even when ion concentrations are low. The inner cylinder of each analyser is divided into four isolated parts which maintain a constant voltage during a measurement cycle. The outer cylinder is divided into 21 isolated rings connected to 21 electrometers. Naturally charged particles are moved by a radial electric field from the inner cylinder of the DMA to the outer cylinder. The current carried by the ions is further amplified and measured with electrometers. Each measurement cycle is followed by an offset measurement during which particles in the sample air are charged by a unipolar corona charger and electrically filtered. During the whole measurement period and for all three instruments, the offset cycle was at least as long as the measurement cycle to ensure a good signal to noise ratio.

2.3 Radon measurements

Radon at Puy de Dôme is measured with the active deposit method (Polian et al., 1986; Biraud et al., 2000). The method is based on the measurement of ^{222}Rn daughters (^{218}Po, ^{214}Bi, ^{214}Po) which are absorbed onto atmospheric particles. Total active deposits of those daughters are accumulated on a cellulose filter during one hour (air is sampled on the roof of the station, 11m above the ground). Then the filter is automatically moved under one alpha detector coupled to a photo-multiplicator. Total α radioactive decay is measured every 10 min over the span of one hour. The measurement error is estimated to be 10 to 20 % (Polian et al., 1986). A correction is performed on the calculated ^{222}Rn activities to consider the radioactive disequilibrium between ^{222}Rn and its short-lived daughters. A disequilibrium factor of 1.15, like the one estimated by Schmidt (1999) for a similar mountain station at Shauinsland, Germany, was used for correcting the data.

2.4 Auxiliary measurements

In addition to the AIS size distributions, auxiliary measurements were used in the current study. Routine meteorological parameters such as wind speed and direction, temperature, pressure and relative humidity are continuously recorded at the station. The aerosol particle number size distributions (10–420 nm) were measured with a Scanning Mobility Particle Sizer (SMPS). The hygroscopic properties of the aerosol particles were obtained from a Hygroscopic Tandem Differential Mobility Analyser (HTDMA). The SMPS and the HTDMA are both custom-built instruments and were operating behind a Whole Air Inlet (WAI) with a cut-off size of 30 µm. More detailed explanations on the SMPS and the inlet system can be found in Venzac et al. (2009) and complementary information on the HTDMA is available in Duplissy et al. (2009). In-cloud conditions were filtered out by using either liquid water content (LWC) measurements or RH data when LWC measurements were not available. The limit value

RH = 98 % was used to distinguish in-cloud and out-of-cloud conditions.

2.5 Data analysis

2.5.1 The simplified balance equation for small ions

The initial balance equation for the small ions concentration originates from Israël (1970):

$$\frac{dn_{\pm}}{\mathrm{d}t} = Q_{\pm} - \alpha n_{\pm} n_{\mp} - n_{\pm} \int_{d_\mathrm{p}} \sum_{q=-\infty}^{\infty} \beta_{\pm}(d_\mathrm{p}, q) N(d_\mathrm{p}, q) d d_\mathrm{p}, \quad (1)$$

where $Q_{\pm}$ is the positive or negative ion production rate, $n_{\pm}$ is the concentration of positive or negative small ions, α is the ion-ion recombination coefficient, $\beta_{\pm}(d_\mathrm{p}, q)$ is the small ion-aerosol particle attachment coefficient, q is the charge of the aerosol particle and $N(d_\mathrm{p}, q)$ is the concentration of aerosol particles. Equation (1) can be simplified under the assumptions that there are (1) small ions in a bipolar environment, (2) equal concentrations of negative and positive small ions, and (3) symmetrical charging of aerosol particles. The resulting simplified balance equation for cluster ions concentration is given by Hoppel et al. (1986):

$$\frac{dn}{\mathrm{d}t} = Q - \alpha n^2 - \beta_{\mathrm{eff}} N_{\mathrm{tot}} n, \quad (2)$$

where n is the cluster ions concentration, β_{eff} is the effective ion-particle attachment coefficient and N_{tot} is the total aerosol particle concentration. Two processes responsible for the loss of small ions are taken into account in Eq. (2). The first is the ion recombination (αn) while the second represents the adsorption of small ions onto aerosol particles ($\beta_{\mathrm{eff}} N_{\mathrm{tot}}$) and will be referred to as "aerosol ion sink" (S_a) in the following sections. The calculation of the ion recombination sink was done using the common average value of $1.5 \times 10^{-6}\,\mathrm{cm^3\,s^{-1}}$ for coefficient α in continental areas (Hoppel et al., 1986). The loss of ions by ion-induced nucleation is not considered in the balance equation for small ions. In the case of steady state, the ionization rate can be derived from Eq. (2):

$$Q = \alpha n^2 + \beta_{\mathrm{eff}} N_{\mathrm{tot}} n. \quad (3)$$

The aerosol ion sink was calculated using a simple approximation function from Tammet (1991) and further improved by Hõrrak et al. (2008) for the single size ion-aerosol attachment coefficient $w(d_\mathrm{p})$:

$$S_\mathrm{a} = \beta_{\mathrm{eff}} N_{\mathrm{tot}} = \int_{d_\mathrm{p}} w(d_\mathrm{p}) N(d_\mathrm{p}) d d_\mathrm{p}$$

$$= \int_{d_\mathrm{p}} \sqrt{\frac{d_\mathrm{p} - 1\,\mathrm{nm}}{d_\mathrm{p} + 5\,\mathrm{nm}}} \frac{d_\mathrm{p}}{40\,\mathrm{nm}} 10^{-6} N(d_\mathrm{p}) d d_\mathrm{p}, \quad (4)$$

where the aerosol particle diameter d_p is given in nanometers. In this study, the aerosol ion sink was calculated by exclusively using the SMPS aerosol size distribution (10–420 nm). This can be argued for by the fact that the median contribution of larger particles (0.45–17.5 µm) to the ion sink (calculated between February 2010 and December 2011 from an Optical Particle Counter (OPC) size distributions) only represented a fraction of 1.23 % and 2.08 % of the sink derived from the SMPS, when considering dry and wet diameters, respectively. The same observation was reported by Hõrrak et al. (2008) in Hyytiälä, Finland.

2.5.2 Nucleation events classification

The classification of event days was achieved visually using the contour plot of the positive and negative ion size distributions. Data were first separated into three main groups: undefined, non-event and nucleation event days according to Dal Maso et al. (2005). A closer analysis suggested by Yli-Juuti et al. (2009) and based on previous work by Hirsikko et al. (2007a) and Vana et al. (2008) was then performed to classify event days into different classes (Ia, Ib, II and Bump) according to their applicability to a growth rate and a nucleation rate analysis:

- Ia: a continuous growth is observed from the cluster size (0.5 nm) up to particles larger than 20 nm;
- Ib: these events are weaker than Ia events and the growth may be interrupted on some size ranges but the growth rate analysis remains possible;
- II: an event is clearly detected but the growth is definitely not regular and the shape of the size distribution evolution is unclear. Further analysis of the event characteristics is complicated or impossible;
- Bump: a burst of clusters is visible but it is not followed by a significant growth and particle formation process.

3 Results and discussion

3.1 New particle formation event statistics

The purpose of this section is only to discuss new particle formation (NPF) event frequency and type at the PDD station in order to further examine the behaviour of cluster ions on event and non-event days in the next sections. Formation and growth rate analysis are beyond the scope of this paper and were performed in Boulon et al. (2011).

The monthly mean NPF event frequency at the Puy de Dôme is presented in Fig. 1, initially considering the whole data set (in-cloud measurements will be excluded in the next sections). A summary of the classification of the days into event, non-event and undefined categories according to the

Table 1. Statistics on event, non-event and undefined days observed at the Puy de Dôme (February 2007–February 2012). In case of event days, additional statistics concerning the type of event are reported.

	NPF event days						Non-event days	Undefined days
	Number	Frequency (%)	Type of event (%)				number	number
			Ia	Ib	II	Bump		
Winter	85	18	7	18	45	29	88	2
Spring	117	25	11	32	33	24	111	2
Summer	122	27	8	7	19	66	122	4
Fall	109	24	8	21	30	40	78	2
All seasons	433	23	9	20	29	39	414	10

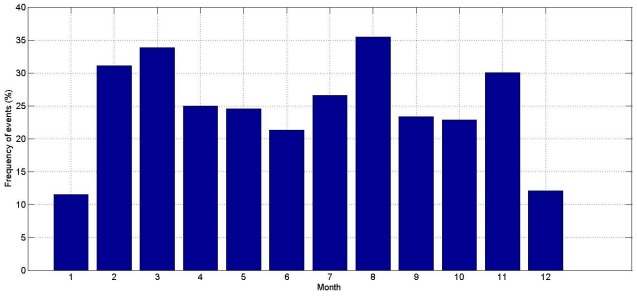

Fig. 1. Monthly mean nucleation frequencies at the Puy de Dôme. February 2007–February 2012, Puy de Dôme.

season and for the whole measurement period is given in Table 1. The NPF event frequency on the entire data set was around 23.4 %, which is somewhat smaller than previously reported (30.8 %) in the studies by Boulon et al. (2011) or Venzac et al. (2007), performed on shorter time periods. In the present study, it was possible to distinguish three maxima with frequencies equal or greater than 30 % (one in late winter/early spring, one in summer and one in late fall); in the previous work from Boulon et al. (2011), the same pattern was observed but the maxima were slightly higher (around 40 %) and they were obtained earlier in the summer and fall. Despite the fact that the influence of the event classification on cluster ion characteristics will not be deeply discussed later in this study, the frequency of each class is given according to the season and for the entire data set as additional information in Table 1. Considering all the seasons, Ia events are rare since they represent on average only 8.8 % (7.1–11 %) of all events. In winter and spring, class II events are dominant with 44.7 and 33.1 %, respectively, while in summer and fall, "bump-type" events are predominant with 65.6 and 40.4 %, respectively. When considering the whole measurement period, "bump-type" events occur most frequently, representing 39.3 % of the events detected at the station. At altitude sites such as the Puy de Dôme, air masses might not be homogeneous over the whole diurnal cycle, as they are influenced alternatively by boundary layer (BL) air masses and free tropospheric air masses. Moreover, the presence of clouds is frequent at the station, eventually interrupting the NPF process. Hence, the aerosol particle growth during the NPF process is likely to be less regular than at BL stations.

The influence of several atmospheric parameters as well as air mass back trajectories on NPF event characteristics at the Puy de Dôme was previously studied by Boulon et al. (2011). Only the relative humidity, the ozone concentration and the condensation sink showed significant differences between NPF and non-NPF event days, with lower values on event days. The link between the occurrence of NPF events and cluster ion properties will be discussed in the following sections.

3.2 Cluster ion concentration and size

It is first important to note that during the five-year measurement period, no discontinuities in the cluster ion concentration that could be explained by the use of three different instruments at two different places were detected. Figure 2 shows the annual variation of the median concentration of the positive (upper panel) and negative (bottom panel) cluster ions obtained after filtering out the cloudy conditions. Based on the five-year measurement period, both positive and negative cluster ions are always present at the Puy de Dôme and their monthly-median concentrations display similar annual trends, with lower values in late winter – early spring. Negative ion concentrations are on average slightly higher than positive ones and they also spread over a larger range of values, but considering the two polarities, the monthly-median concentrations typically vary between 200 and 600 cm^{-3}. For positive ions, the highest monthly-median concentration is 569 cm^{-3} in November whereas the lowest is in March (229 cm^{-3}). For negative ions the highest concentration is 566 cm^{-3} in August while the lowest is 189 cm^{-3} in February. These values are in agreement with the previous study made by Venzac et al. (2007).

Cluster ions appear to be ubiquitous in the atmosphere, and this observation is not specific to the Puy de Dôme (Hirsikko et al., 2011). A permanent pool of cluster ions was observed in other high-altitude sites (Boulon et al., 2010), as well as in coastal stations (Vana et al., 2008; Komppula et al., 2007) or in continental areas (Kulmala and Kerminen, 2008; Manninen et al., 2009). The annual variation of the cluster

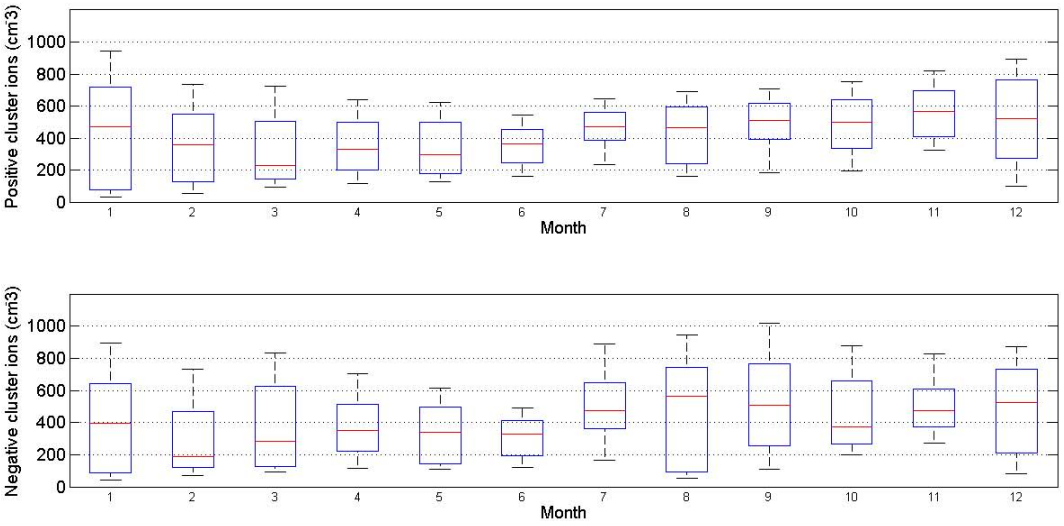

Fig. 2. Annual variation of cluster ion (0.8–1.9 nm) concentration. Red line represents the median value, bottom and top sides of the blue boxes symbolize the 25th and 75th percentile, respectively, and the extremities of the black lines stand for the 10th and 90th percentile. Statistics are based on hourly median concentrations. February 2007–February 2012, Puy de Dôme.

ion concentration at the Puy de Dôme is similar to the annual variation of positive cluster ions described by Boulon et al. (2010) at the high-altitude station of Jungfraujoch, Switzerland, but it differs from the annual variation observed in Hyytiälä, which displays two maxima in August and October, and two minima in February and July (Hirsikko et al., 2005). Moreover, cluster ion concentrations recorded at the Puy de Dôme are in general slightly lower than the concentrations measured in Hyytiälä (200–1500 cm^{-3} for both polarities). However, cluster ion concentrations in spring at the Puy de Dôme are comparable to the concentrations reported by Komppula et al. (2007) for the coastal station of Utö, Finland ($250 \pm 110\,cm^{-3}$ for positive ions, $280 \pm 120\,cm^{-3}$ for negative ions).

We further investigated the cluster ion concentrations separately for the different seasons. The entire data set includes the equivalent of 842 available days of measurement in clear sky conditions which are distributed over the seasons as follows: 175 days in winter, 230 in spring, 248 in summer and 189 in fall. Furthermore, days were classified as "event day" or "non-event day" according to the detection of an NPF event or not and were analysed independently. Table 2 presents the ratio of the positive ion concentration to the negative ion concentration and the correlation between the concentrations of the two polarities. Table 3 gives more detailed statistics on positive and negative cluster ion concentrations separately for event and non-event days. The concentrations of positive and negative cluster ions are relatively closely correlated and the correlation is in general better on event days, with determination coefficients ranging between 0.38 and 0.87 in different seasons. However, the correlation is not as strong as the correlation of 93.6 % reported by Hõrrak et al. (2008) in Hyytiälä.

Table 2. Median values of the ratio of positive to negative hourly median cluster ions (0.8–1.9 nm) concentration (r) and determination coefficients between positive and negative cluster ions concentration (R^2). February 2007–February 2012, Puy de Dôme.

Season	Event days		Non-event days	
	r	R^2	r	R^2
Winter	1.02	0.84	1.01	0.72
Spring	0.93	0.87	0.88	0.73
Summer	0.97	0.52	0.91	0.53
Fall	0.92	0.38	0.86	0.55
All seasons	0.96	0.63	0.91	0.66

It can also be seen from Table 2 and Table 3 that negative ion concentrations are in general slightly higher than positive ones, with an exception during the winter season which displays very similar concentrations for the two polarities. It is worth noticing that this difference is smaller on event days, which display ratios of positive to negative cluster ion concentrations higher than 0.90 in all seasons. This result is in agreement with the previous study by Venzac et al. (2007) at the Puy de Dôme and supports other observations in different environments, for example Mace Head, Ireland (Vana et al., 2008) or Utö (Komppula et al., 2007). However, these observations differ from what was reported from other stations, for example Tahkuse, Estonia, where both Komppula et al. (2007) and Hõrrak et al. (2003) detected higher positive cluster ion concentrations. At the Jungfraujoch station, lower negative cluster ion concentrations were also reported by Vana et al. (2006). According to the authors, lower pressure conditions at high altitude increased the mobility of cluster ions, which could eventually exclude the smallest clusters

Table 3. Statistics of the positive and negative cluster ion mode (0.8–1.9 nm) concentration (n_+ and n_-, respectively) and mean diameter (d_+ and d_-, respectively) in clear sky conditions. Calculations are based on hourly medians. February 2007–February 2012, Puy de Dôme.

Winter						
	NPF event days			Non-event days		
	Median	25th %	75th %	Median	25th %	75th %
n_+, cm^{-3}	505	343	724	340	77	679
n_-, cm^{-3}	525	194	697	232	87	585
d_+, nm	1.266	1.095	1.279	1.223	1.099	1.276
d_-, nm	0.964	0.889	1.029	0.944	0.891	0.991
Spring						
	NPF event days			Non-event days		
	Median	25th %	75th %	Median	25th %	75th %
n_+, cm^{-3}	392	255	597	322	193	495
n_-, cm^{-3}	428	303	609	359	225	514
d_+, nm	1.256	1.209	1.297	1.247	1.010	1.302
d_-, nm	0.953	0.875	1.010	0.912	0.846	0.972
Summer						
	NPF event days			Non-event days		
	Median	25th %	75th %	Median	25th %	75th %
n_+, cm^{-3}	511	388	614	435	334	528
n_-, cm^{-3}	496	330	705	453	332	633
d_+, nm	1.273	1.175	1.333	1.256	1.134	1.328
d_-, nm	1.023	0.911	1.079	0.984	0.907	1.044
Fall						
	NPF event days			Non-event days		
	Median	25th %	75th %	Median	25th %	75th %
n_+, cm^{-3}	537	398	658	435	334	528
n_-, cm^{-3}	461	292	714	497	300	772
d_+, nm	1.239	1.086	1.282	1.256	1.134	1.328
d_-, nm	0.974	0.90	1.034	0.970	0.877	1.039
Whole measurement period						
	NPF event days			Non-event days		
	Median	25th %	75th %	Median	25th %	75th %
n_+, cm^{-3}	502	343	641	435	334	528
n_-, cm^{-3}	474	296	679	409	230	616
d_+, nm	1.253	1.125	1.302	1.234	1.088	1.295
d_-, nm	0.976	0.889	1.042	0.952	0.863	1.020

from the measurement range of the instrument (especially in negative mode).

The fact that at the Puy de Dôme negative ions are, with the exception of winter, slightly more numerous than positive ones, contrasts with what would be expected from the atmospheric electrode effect. Indeed, this effect predicts that in fair weather, higher positive cluster ion concentrations should be detected near the ground and up to a few meters because of the negative charging of the Earth (Hoppel et al., 1986). At the Puy de Dôme, horizontal and vertical winds from the valley are often observed. This turbulence mixes the air, which may hide or suppress the effect of the electric field, and thus partly explain why positive ions are not found to be predominant.

Figure 3 shows the diurnal variation of the positive ion concentration for the different seasons and separately for event and non-event days. No distinct diurnal variation is observed for any of the seasons on non-event days. However, on event days, positive cluster ion concentration displays a maximum around 12:00 UTC time (−1 h local winter time) and

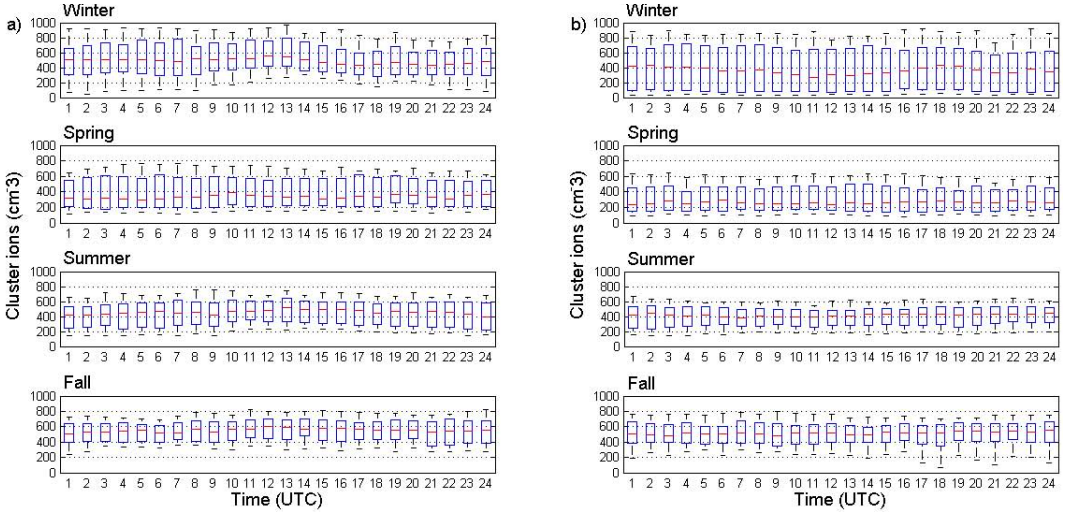

Fig. 3. Diurnal variation of positive cluster ion (0.8–1.9 nm) concentration on **(a)** event days and **(b)** non-event days. Red line represents the median value, bottom and top sides of the blue boxes symbolize the 25th and 75th percentile, respectively, and the extremities of the black lines stand for the 10th and 90th percentile. February 2007–February 2012, Puy de Dôme.

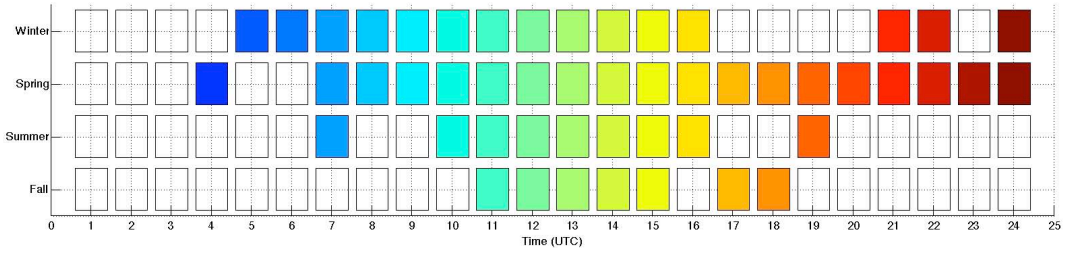

Fig. 4. Result of the Mann–Whitney U test applied on positive cluster ion concentration from event and non-event days. Squares are colored when the null hypothesis of samples with different medians cannot be rejected at the threshold of 5 %. February 2007–February 2012, Puy de Dôme.

on average, the concentrations appear to be slightly higher compared to non-event days. For negative cluster ions (figure not shown) it is hard to distinguish any clear diurnal variation of the concentration, both on event and non-event days. The major difference between event and non-event days can be seen in winter and spring, which exhibit higher positive cluster ion concentrations during the whole day (Table 3). In spring, the concentrations are increased by a factor in the range of 1.10–1.47 on event days and in winter the increase is even more pronounced with factors in the range of 1.51–2.86.

In order to verify these last statements, the differences in cluster ion concentrations recorded on event and non-event days were tested with the Mann–Whitney U test. Figure 4 shows that for positive ion concentrations, the null hypothesis of samples with different medians cannot be rejected at the threshold of 5 %, at least during the time period 10:00–16:00 UTC over all seasons. This means that on event days, positive cluster ion concentrations are significantly higher than on non-event days. This is the case during almost the whole day in winter and spring and on a more restricted time period in summer and fall. The last observation can be related to the fact that "bump-type" events are predominant in summer and fall. Indeed, it appears that in the case of "bump-type" events, in all seasons, the positive cluster ions concentration displays clear differences on a well-defined and restricted period during the day compared to non-event days. The most significant differences between event and non-event days are in winter between 10:00 and 16:00 UTC with cluster ion concentrations 1.24 to 1.92 times higher on event days. The lowest differences are in fall with small ion concentrations increased by a factor in the range 1.08–1.20 during event days compared to non-event days. For the negative ions, the U test confirms that the concentrations between event and non-event days are significantly different only in winter and spring.

Several articles have already reported higher positive cluster ion concentrations on event days, but none of them mentioned the use of a statistical test to confirm their observation. Boulon et al. (2010) found that positive ion concentrations

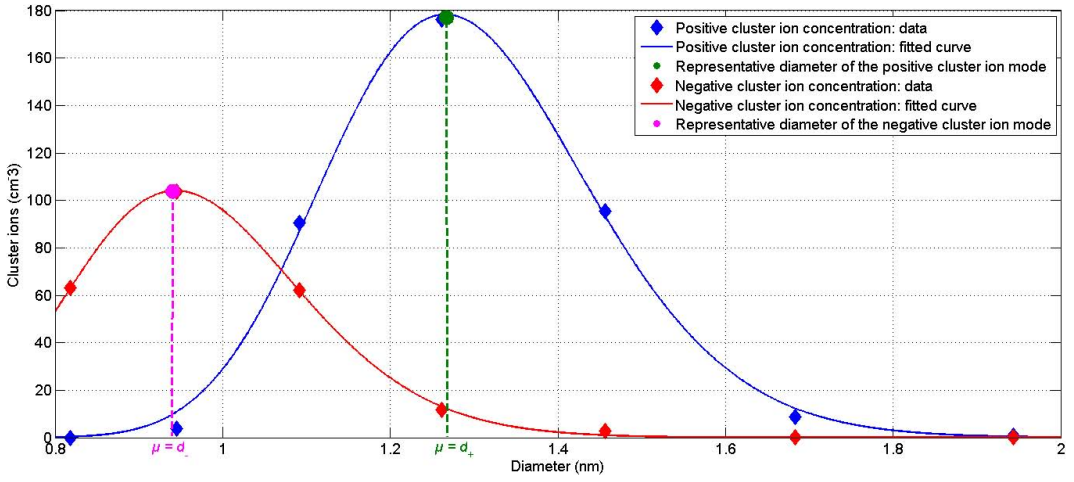

Fig. 5. Determination of the representative diameters of the positive and cluster ion mode (d_+ and d_-, respectively) by fitting a log-normal distribution to the cluster ion size distribution. d_+ (respectively d_-) corresponds to the location parameter (usually referred to as "μ") of the corresponding log-normal distribution.

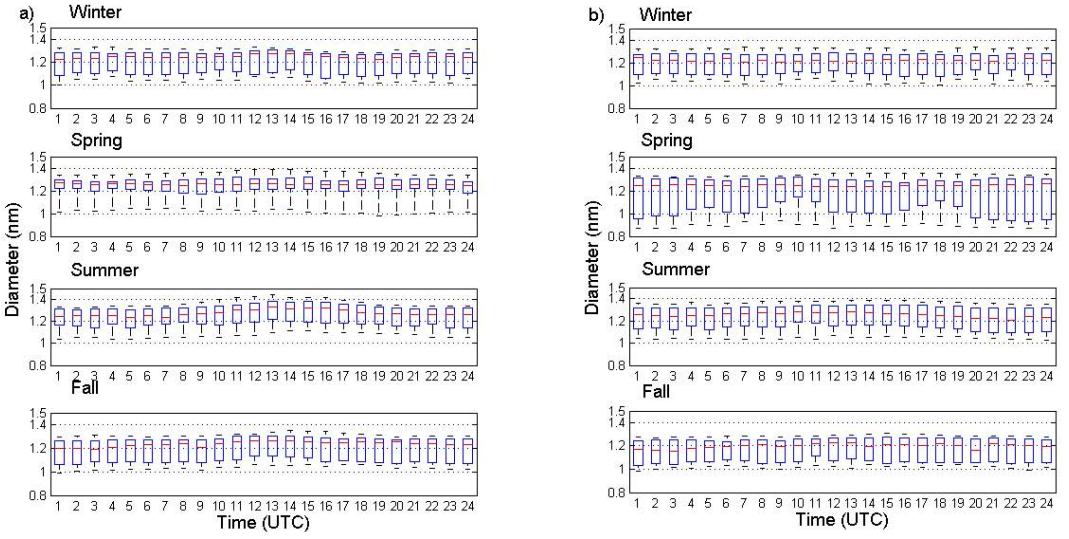

Fig. 6. Diurnal variation of the positive cluster ion mode (0.8–1.9 nm) diameter on **(a)** event days and **(b)** non-event days. Red line represents the median value, bottom and top sides of the blue boxes symbolize the 25th and 75th percentile, respectively, and the extremities of the black lines stand for the 10th and 90th percentile. February 2007–February 2012, Puy de Dôme.

increased on average by a factor of 1.5 on event days between 09:00 and 12:00 local time (LT) at the Jungfraujoch (JFJ) station. Hõrrak et al. (2008) measured average positive ion concentrations of 530 cm^{-3} on NPF event days versus 424 cm^{-3} on non-event days in Hyytiälä in spring.

The diurnal variation of the positive cluster ion concentration with a stable minimum at night and a maximum around noon observed at the Puy de Dôme seems to be representative of high-altitude sites (Boulon et al., 2010), but it is clearly different from the diurnal variation observed in BL sites. In Tahkuse, the positive cluster ion concentration displayed a maximum in the early morning (06:00–07:00 LT) and a minimum around 18:00 LT (Hõrrak et al., 2003); moreover, this diurnal variation was more evident during the warm season, between April and September. The same pattern for the diurnal variation of the cluster ion concentration with a maximum during night time was reported for Hyytiälä (Hõrrak et al., 2008) and K-Puszta, Hungary, in late spring (Yli-Juuti et al., 2009). For these three BL stations, it is likely that small ion concentration and radon activity have similar temporal variations. One should note that the dynamics of the BL can also impact the cluster concentration itself, by a concentration or dilution effect of cluster ions in the observed volume.

On the contrary, at high-altitude sites, the influence of surface emissions (including radon) is higher during the daytime when the BL reaches the station or when katabatic winds

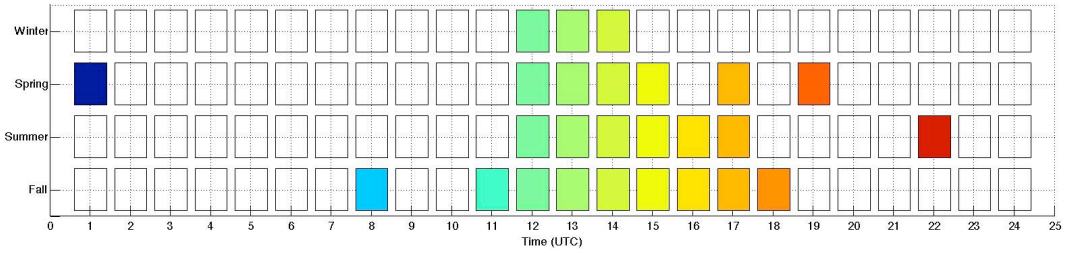

Fig. 7. Result of the Mann and Whitney U test applied on the positive cluster ion mode diameter from event and non-event days. Squares are colored when the null hypothesis of samples with different medians cannot be rejected at the threshold of 5 %.

bring valley breezes to the station (Boulon et al., 2010). For the studies which focused on both positive and negative ions, the authors did not mention significant differences between the diurnal variations of the concentrations of the two polarities (e.g. Yli-Juuti et al., 2009). The dissimilarity in the different diurnal variations between the two polarities at the Puy de Dôme, especially in summer and fall on event days, however indicates that positive and negative cluster ions could be concerned by nucleation, but with unequal involvements in the process.

In order to study the evolution of the small ion mean size, a log-normal distribution was fitted to the hourly median cluster ion size distributions to obtain the representative diameter of the mode. This diameter corresponds to the location parameter of the log-normal distribution (usually referred to as "μ" in the literature). In the following, the representative diameter of the cluster mode will be referred to as d_+ and d_- for positive and negative ions, respectively. An illustration of the fitting process for the determination of d_+ and d_- is given in Fig. 5. Table 3 reports statistics of mean diameters for the two polarities separately for event and non-event days. Negative ions appeared to be significantly smaller than positive ones as d_+ was typically in the range 1.2–1.3 nm, while d_- was in the range 0.9–1.1 nm.

Figure 6 shows the diurnal variation of d_+ separately for the different seasons and for event and non-event days (figure not shown for d_-). For positive ions, no major difference can be seen between the different seasons, whereas for negative ions, the diameters are smaller in winter and spring, especially on non-event days (Table 3). On event days, the diurnal variation of d_+ shows a maximum around noon, which is not detected on non-event days; as a consequence, the diameter of the cluster mode is significantly larger around noon on event days (Figs. 6 and 7) compared to non-event days. For negative ions, no diurnal variation in the median diameters can be seen except on event days in summer with a significant maximum around noon, which displays median values increased by a factor of 1.09 compared to hourly morning median values.

The result of the U test applied on negative ion diameters shows that these differences between event and non-event days are statistically confirmed in summer. The U test also exhibits some differences in winter and spring. However, especially in winter, the differences are only observed on very short time periods during the day and they do not match well with the time period during which the NPF process takes place. Thus, this observation suggests the link between the NPF process and the increase of the negative ion size is weak, whereas it appears to be potentially stronger in the case of positive ions. A possible explanation could rely on the different chemical compositions of the two polarities but an accurate chemical analysis would be necessary to confirm this hypothesis.

Similar cluster ion diameters were reported by Manninen et al. (2009) in Hyytiälä (1.1–1.3 nm), with slightly smaller values for the negative polarity. Boulon et al. (2010) observed an increase in the cluster ion concentration and a shift of the cluster ion mode diameter to larger sizes during the new particle formation processes on event days at the Jungfraujoch station. Based on these observations, the authors suggested that the formation of new clusters occurred during NPF events.

We have demonstrated so far that at the Puy de Dôme, positive and negative cluster ions showed different behaviours, both in terms of concentration and size. Particularly, contrary to observations reported from some previous studies (Wilhelm et al., 2004; Laakso et al., 2007; Enghoff and Svensmark, 2008), at the Puy de Dôme, positive cluster ions exhibited more variation in their properties (concentration and size) between event and non-event days compared to negative ones. This observation suggests that positive cluster ion characteristics might be more significantly impacted by the occurrence of a NPF event than negative ones. Hence, we will now focus exclusively on positive cluster ions for the rest of the present study.

First, since event days are characterized by an increase of both the positive cluster ion concentration and mode diameter, we shall investigate if the increase of the concentration is not a consequence of the increase of the cluster diameter. Indeed, the measured small ion concentrations could increase on event days, not because the concentration of the cluster ion mode is changing but only because the fraction detected by the instrument is larger since ions are getting bigger. Figure 8 shows the hourly median cluster ion mode size

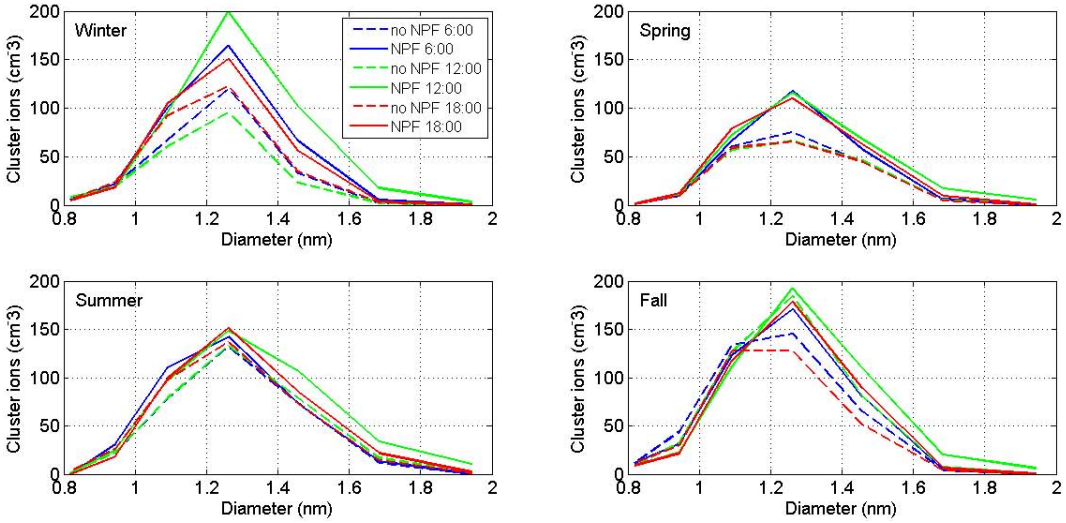

Fig. 8. Positive cluster ion mode size distribution. Blue, green and red curves correspond to 06:00, 12:00 and 18:00 UTC hourly median concentration, respectively. Continuous lines are used for event days and dashed lines for non-event days. February 2007–February 2012, Puy de Dôme.

distribution at 06:00, 12:00 and 18:00 UTC on event and non-event days. The critical size range to study in order to reject the possibility of an artificial increase of the cluster ion concentration due to the sizing limit of the AIS is in the left most part of the size distribution. The small ion concentration corresponding to the diameter 0.82 nm does not show any important diurnal variation on event days compared to non-event days; for this size class, the most significant change is observed on event days in winter when the hourly median small ion concentration rises from 6.18 cm^{-3} at 06:00 to 7.99 cm^{-3} at 12:00 UTC. Even in this case, the increase is far too weak to explain the global increase of the cluster ion concentration on event days. Thus, an artificial increase of the cluster ion concentration due to sizing limits of the instrument can be rejected.

Most of the modifications on the size distribution are observed for ions larger than 1.26 nm. On event days during the time period 06:00–12:00 UTC, the concentration of small ions in the size range 1.26–1.94 nm is increased by a factor between 1.14 in spring and 1.36 in winter. For the same size range, ion concentrations are decreased by factors in the range 1.13 (spring) – 1.53 (winter) between 12:00 and 18:00 UTC and the resulting size distribution is very similar to the size distribution at 06:00 UTC. These observations suggest that both formation and growth of positive cluster ions do occur during the nucleation process on event days in the morning; a large fraction of these clusters is then lost later in the afternoon (the effect of different sinks will be discussed in the next section). At the Jungfraujoch station, Boulon et al. (2010) also reported a shift of the positive cluster mode diameter to larger sizes and an increase of the positive cluster ion concentration on event days. Hence it seems that, at least for high-altitude stations, NPF events do have specificities in terms of both the size and the concentration of positive small ions.

3.3 Positive cluster ion loss and production

3.3.1 Dry and wet sink due to background aerosol

The sink due to background aerosol, referred to as aerosol ion sink, was first estimated by using the dry diameters of the SMPS size distribution. For each season, Fig. 9 represents the median diurnal variation of the dry aerosol ion sink (Sa_{dry}) on the left plot and hourly median size distribution of the aerosol ion sink at 06:00, 12:00 and 18:00 UTC on the right plot. The lowest dry aerosol ion sinks are in the range of 1.19×10^{-3}–3.75×10^{-3} s^{-1} in winter while the highest are in the range of 4.62×10^{-3}–8.87×10^{-3} s^{-1} in spring. In winter and fall, the dry sink shows the same diurnal pattern, being almost constant until 12:00 UTC with comparable values on event and non-event days. The diurnal variation of the dry sink displays a maximum around 15:00 UTC on non-event days and later at 17:00–18:00 UTC on event days. During the afternoon, the sink is increased by a factor of 1.93, both on event and non-event days in fall, while in winter the increase is even more important on event days (a factor of 3.16 on event days versus 1.68 on non-event days). Concerning spring and summer, the sink seems to be higher on non-event days, but this observation will be discussed in the following section using the U test. The diurnal variation of the dry sink shows a minimum around 07:00 UTC and a maximum at 11:00 UTC on non-event days; the maximum is reached later on event days, after 15:00 UTC. The maximum sink value is typically 1.3–1.4 times higher than the

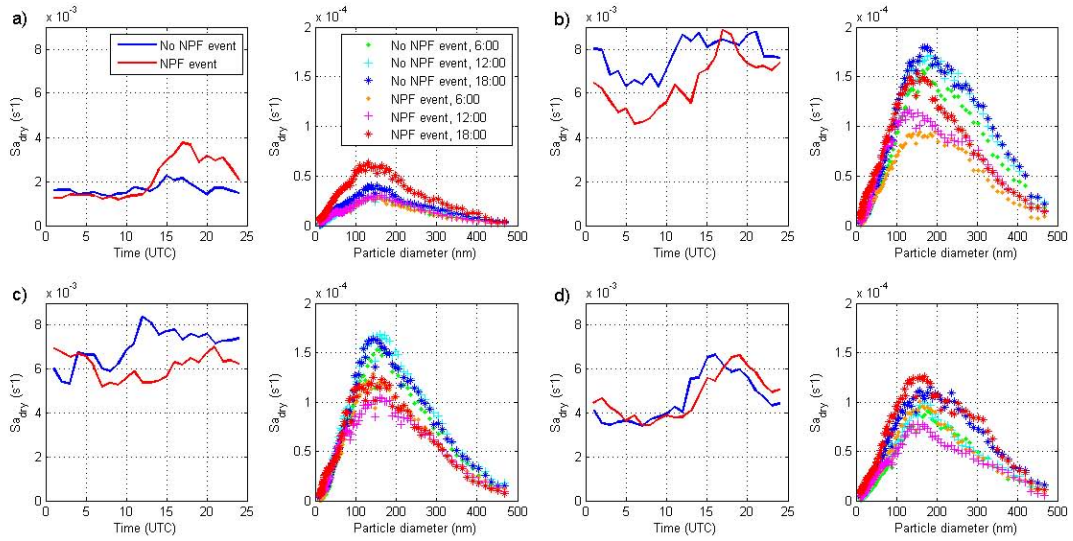

Fig. 9. Aerosol ion sink based on dry SMPS size distribution in **(a)** winter, **(b)** spring, **(c)** summer and **(d)** fall. For each season, the figure on the left represents the diurnal variability of the median sink; the figure on the right represents the hourly median size distributions of the sink at 06:00, 12:00 and 18:00 UTC. February 2007–February 2012, Puy de Dôme.

minimum value. The most significant difference is on event days in spring, with multiplying factors around 1.9.

The diurnal variations of the dry aerosol ion sink discussed above are comparable to the diurnal variations of the CPC median concentrations reported by Venzac et al. (2009) at the Puy de Dôme. On event days, the increase of the ion sink during the daytime can mainly be attributed to the NPF process, while on non-event days it is more likely the pre-existing aerosol particles contained in the BL reaching the site which are responsible for the increase of the ion sink during the afternoon. This last hypothesis is supported by the size distributions of the aerosol ion sink presented in Fig. 9. Except in fall, the three hourly median size distributions from non-event days superimpose well with each other, which signifies that the size distribution of the dry sink does not evolve during the daytime. Thus, the increase of the ion sink is not linked to a growth process of aerosol particles. On the contrary, we can observe that on event days, the ion sink size distribution measured at 18:00 UTC significantly differs from the size distributions measured at 06:00 and 12:00 UTC, especially in winter and fall. The contribution of the largest particles to the sink increases throughout the day. This suggests that on event days the NPF process mostly influences the sink variations with particle growth.

Since the effect of the hygroscopic growth of aerosol particles has been reported to be significant on aerosol ion sink and further on ionization rate calculations by Hõrrak and coworkers (2008), we made new calculations of the aerosol sink by calculating wet diameters from the SMPS size distribution. In order to estimate the dependence on ambient relative humidity (RH) of the hygroscopic growth factor (GF) of aerosol particles, we used a parameterization originating from Zhou et al. (2001) and already used in several studies (Hõrrak et al., 2008; Laakso et al., 2004):

$$\mathrm{GF} = \frac{d_{\mathrm{wet}}}{d_{\mathrm{dry}}} = \left(1 - \frac{\mathrm{RH}}{100}\right)^{\gamma}. \quad (5)$$

The exponent γ is a function of particle size and was parameterized from the particle GF measurements of monodisperse aerosol samples (25, 35, 50, 75, 110, 165 nm) at RH = 90 % carried out at the Puy de Dôme during the period October 2008 – December 2012. Gamma parameterizations are given for each season in Table 4.

Table 4. Coefficients of the gamma parameterization written as $\gamma = -a\frac{d_{\mathrm{p}}}{1\,\mathrm{nm}} - b$. R^2 is the determination coefficient between the γ obtained from GF measurements and the corresponding parameterized values.

Season	$a(\times 10^{-4})$	$b(\times 10^{-2})$	R^2
Winter	3.944	6.694	0.9920
Spring	5.603	6.796	0.9628
Summer	5.505	7.369	0.9861
Fall	4.712	9.285	0.9960

The resulting values of the growth factor are shown in Fig. 10 and compared to measurements carried out at the Puy de Dôme at different relative humidities (40 %, 60 %, 80 % and 90 %) during the same time period. As one could expect, at RH = 90 %, the parameterization fits well with the measurements. Decreasing the RH, the calculation and measurement do not match well. Several hypotheses can be proposed to explain this gap: (1) gamma parameterization is obtained at RH = 90 %, which can lead to some discrepancies for lower

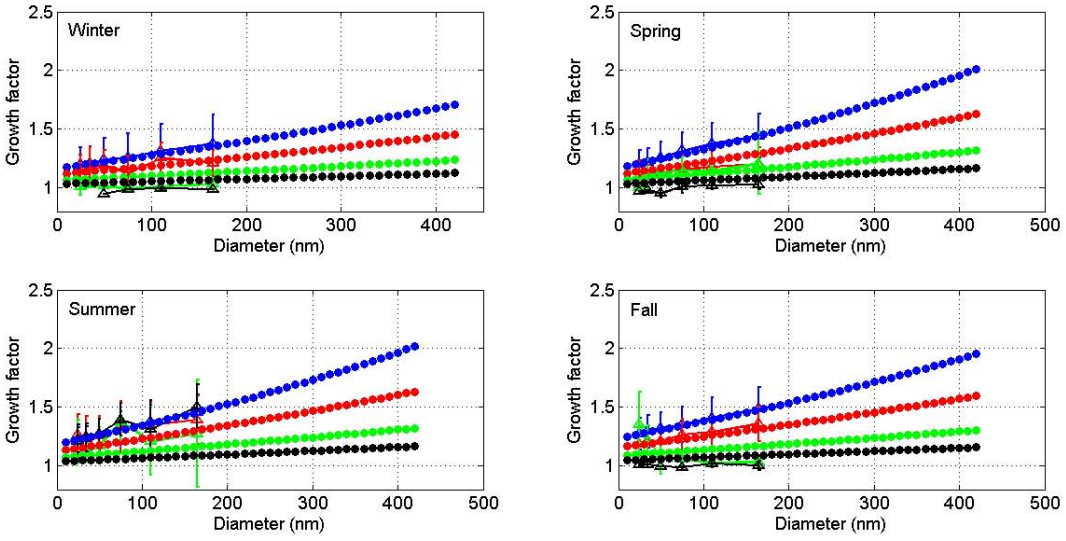

Fig. 10. Growth factor parameterization as a function of particle size and relative humidity (black = 40 %, green = 60 %, red = 80 %, blue = 90 %). Mean measurements and standard deviation are given for the comparison (triangles); the colours correspond to different relative humidities and respect the code previously defined. February 2007–February 2012, Puy de Dôme.

ambient humidity and (2) for RH < 90 %, measurements are very rare, so the comparison must be done carefully. For diameters above 300 nm, we obtain GF values larger than 2 at RH = 90 % in spring and summer, which seems to be slightly overestimated since it is relatively close to the value of 2.4 reported for pure NaCl at d_p = 300 nm (Hämeri et al., 2001).

Because particles larger than 300 nm do not represent the major fraction of the aerosol ion sink (Fig. 9), we assume that the overestimation of the GF for the largest diameters should not dramatically impact our estimations of the wet aerosol ion sink. Based on Fig. 9, the largest contribution to the ion sink comes from particles in the size range 100 - 300 nm, for which we obtain GF values between 1.27 and 1.73 at RH = 90 %. These values appear to be comparable with the values reported by Hämeri et al. (2001) under the assumption of "more hygroscopic particles". For RH > 90 % the parameterization seems to widely overestimate the GF (figure not shown); Hõrrak et al. (2008) also reported that the use of the model was critical for RH > 90 %. Thus, we decided to exclude all the data points corresponding to RH > 90 % when taking into account the effect of the hygroscopic growth in the balance equation for small ions.

Statistical values of the factors of the small ion balance equation, including the wet aerosol ion sink, are presented in Table 5, separately for the different seasons and for event and non-event days. Considering all the measurements, the median wet aerosol ion sink (Sa_{wet}) varies in the range of 1.4×10^{-3}–10.6×10^{-3} s^{-1}. The lowest values are found during the cold season (winter and fall) and the highest values during the warm season (summer and spring). As mentioned before, the increased boundary layer height during the warm season can explain the high values of the ion sink, at least on non-event days. Based on the median values in Table 5, the wet aerosol ion sink appears to be similar on event and non-event days during the cold season whereas during the warm season, the sink is on average increased by a factor of 1.25 on event days compared to non-event days. In order to verify the previous observation, we further investigated the differences of the wet aerosol ion sink between event and non-event days with the U test of Mann and Whitney. It appears that no significant changes in ion sink values can statistically be confirmed for any of the seasons.

3.3.2 Ionization rate calculation from the balance equation

The values of the positive ionization rate (Q) were derived from Eq. (3) and are presented in Table 4. It should be noticed that instead of assuming equal concentrations for positive and negative ions, we used the measured concentrations for each polarity. It can be seen that both positive and negative cluster ion concentrations reported in Table 4 are higher than the concentrations reported in Table 3, which is not surprising since RH > 90 % were filtered out in Table 4. Indeed, fog and high moisture were reported to cause the loss of small ions in many studies (e.g. Venzac et al., 2007; Hõrrak et al., 2008). Considering all the measurements, the median values of the positive ionization rate are in the range 1.58–3.90 cm^{-3} s^{-1}. The lowest values are in winter and spring and the highest values are in summer and fall.

Based on the median values presented in Table 5, the ionization rate displays similar values on event and non-event days for all seasons except summer, which is characterized by median ionization rates 1.18 times higher on non-event days compared to event days. A deeper analysis

Table 5. Statistical values of the wet aerosol ion sink (Sa_{wet}), the ion loss due to ion recombination ($\alpha\ n_+$), the positive and negative cluster ion concentrations (n_+ and n_-, respectively) the total concentration of aerosol particles (N), the ionization rate (Q) and the ratio of ion loss due to recombination to total ion loss ($\alpha\ n_+/(\alpha n_+ + Sa_{wet})$). All the values are given for RH < 90 % and were calculated from hourly medians. February 2007–February 2012, Puy de Dôme.

Winter						
	NPF event days			Non-event days		
	Median	25th perc.	75th perc.	Median	25th perc.	75th perc.
n_+, cm^{-3}	541	403	761	659	424	845
n_-, cm^{-3}	571	320	750	567	279	793
N, cm^{-3}	1103	680	1911	845	445	1382
Sa_{wet}, $10^{-3}\,s^{-1}$	1.9	1.0	3.6	1.4	0.7	3.4
αn_-, $10^{-3}\,s^{-1}$	0.86	0.48	1.1	0.86	0.42	1.2
Q, $cm^{-3}\,s^{-1}$	1.58	1.07	2.63	1.61	1.01	2.39
$\alpha n_- / (\alpha n_- + Sa_{wet})$	29 %	15 %	50 %	30 %	13 %	56 %
Spring						
	NPF event days			Non-event days		
	Median	25th perc.	75th perc.	Median	25th perc.	75th perc.
n_+, cm^{-3}	465	268	622	360	204	518
n_-, cm^{-3}	460	322	626	378	227	538
N, cm^{-3}	3202	1912	4984	2931	1596	4214
Sa_{wet}, $10^{-3}\,s^{-1}$	8.6	5.1	12.9	10.6	6.2	15.9
αn_-, $10^{-3}\,s^{-1}$	0.70	0.49	0.95	0.57	0.34	0.81
Q, $cm^{-3}\,s^{-1}$	2.58	1.24	4.82	2.83	1.38	4.31
$\alpha n_- / (\alpha n_- + Sa_{wet})$	5.9 %	2.6 %	11 %	3.5 %	1.9 %	7.6 %
Summer						
	NPF event days			Non-event days		
	Median	25th perc.	75th perc.	Median	25th perc.	75th perc.
n_+, cm^{-3}	521	412	626	454	367	540
n_-, cm^{-3}	504	346	718	466	347	645
N, cm^{-3}	3252	2353	4184	3531	2444	4304
Sa_{wet}, $10^{-3}\,s^{-1}$	7.8	4.7	10.3	9.9	6.8	13.9
αn_-, $10^{-3}\,s^{-1}$	0.76	0.53	1.1	0.70	0.52	0.97
Q, $cm^{-3}\,s^{-1}$	3.90	2.30	4.82	4.61	3.03	6.40
$\alpha n_- / (\alpha n_- + Sa_{wet})$	5.8 %	3.3 %	9.8 %	5.8 %	3.3 %	8.8 %
Fall						
	NPF event days			Non-event days		
	Median	25th perc.	75th perc.	Median	25th perc.	75th perc.
n_+, cm^{-3}	549	421	659	505	392	626
n_-, cm^{-3}	466	291	726	497	317	777
N, cm^{-3}	2452	1406	3458	2024	1225	3042
Sa_{wet}, $10^{-3}\,s^{-1}$	6.1	3.0	9.6	6.1	2.9	9.7
αn_-, $10^{-3}\,s^{-1}$	0.71	0.44	1.1	0.75	0.48	1.2
Q, $cm^{-3}\,s^{-1}$	3.48	1.98	6.01	3.64	2.19	5.53
$\alpha n_- / (\alpha n_- + Sa_{wet})$	10 %	5.1 %	20 %	11 %	6.2 %	22 %

of the ionization rate with the U test concludes that differences are significant only in summer between 09:00 and 24:00 UTC. The ionization rates at the Puy de Dôme are on average comparable with the ionization rates reported by Komppula et al. (2007) in Utö ($3\,cm^{-3}\,s^{-1}$) and in Tahkuse ($2.6\,cm^{-3}\,s^{-1}$) in spring. They are also similar to the values reported for Hyytiälä by Laakso et al. (2004) in spring ($2.63\,cm^{-3}\,s^{-1}$) or by Schobesberger et al. (2009)

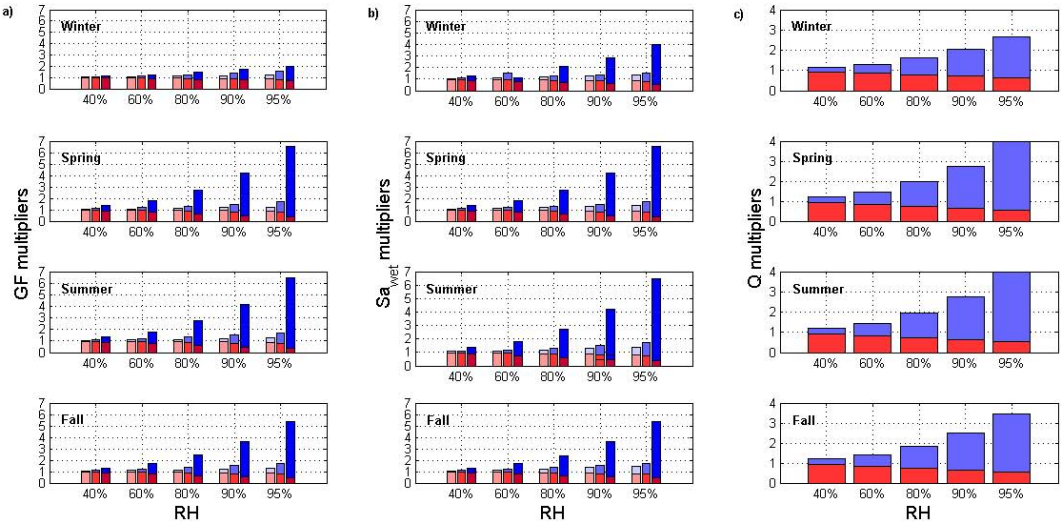

Fig. 11. Sensitivity analysis for **(a)** the growth factor (GF) estimation, **(b)** the wet aerosol ion sink (Sa_{wet}) and **(c)** the ionization rate (Q) when the parameterized γ values are increased by a factor of 2 (blue) or decreased by a factor of 2 (red). Multipliers are given as a function of relative humidity **(a, b, c)** and particle size **(a, b)**. For **(a)** and **(b)** the lightest bars represent the multipliers for the smallest particle diameter (10 nm), the medium bars represent the mean multipliers for the size range 100–300 nm and the darkest bars represent the multipliers for the largest particles (420 nm).

($3.38\,\mathrm{cm^{-3}\,s^{-1}}$ and $3.28\,\mathrm{cm^{-3}\,s^{-1}}$ for positive and negative ions, respectively) for the period March–December 2008.

However, it seems that large discrepancies can occur between ionization rates derived from the small ions balance equation and the measured ionization rates (Franchin, 2009; Schobesberger et al., 2009). For example in Hyytiälä, Laakso et al. (2004) reported measured values 1.7 times higher than calculated values for the same period. As a possible explanation, the authors suggested that some sinks were missing in the balance equation. The loss of ions by ion-induced nucleation or deposition on vegetation could be part of them. Franchin (2009) also suggested that discrepancies between calculated and measured ionization rate could be explained by the chosen range of ions included in the balance equation, since ionization could obviously happen for bigger particles which were not taken into account in the equation.

At the Puy de Dôme, the sink of small ions is often dominated by the aerosol ions sink, but the loss of ions due to ion recombination can represent up to 29 % of the total loss on event days in winter. The values of the recombination sink (αn_-) reported in Table 5 were obtained assuming the recombination coefficient $\alpha = 1.5 \times 10^{-6}\,\mathrm{cm^3\,s^{-1}}$. For the warm season, the ion recombination only represents around 6 % of the total ion loss, which is partly due to the fact that high Sa_{wet} values are recorded at the same time. These fractions are in agreement with the values reported by Tammet (1991) for continental areas.

As previously mentioned in Sect. 3.3.1, growth factor calculations were made under the assumption that the exponent γ was not dependent on ambient relative humidity. Since measured and calculated GF values did not always match well for RH < 90 %, we studied the uncertainty propagation from the gamma parameterization to the calculation of the ion sink and production as a function of humidity (Fig. 11). The sensitivity test is in the form of factors that should multiply the values of the studied parameters when multiplying (blue) or dividing (red) γ values by 2. For the growth factor and the wet aerosol ion sink, the sensitivity is given according to the size of aerosol particles (10 nm, 100–300 nm, 420 nm). All the calculations are detailed in Appendix A.

Figure 11 shows that uncertainties increase with ambient relative humidity but the strongest effect comes from the particle size. For the growth factor and the aerosol ion sink, in the size range below 300 nm the multipliers never exceed 1.72 when using maximum gamma or 0.77 when using minimum gamma at RH = 95 %. However, for all the seasons except winter, high uncertainties are observed for the largest particles (around 420 nm), even at RH = 80 % with multipliers larger than 2 or smaller than 0.6. At RH = 95 % for the same size the multipliers are larger than 6 or smaller than 0.4. Even if Fig. 9 shows that the major contribution to the aerosol ion sink does not come from the largest sizes but from the size range 100–300 nm, the high uncertainties obtained for the largest sizes at RH = 95 % are an additional support for ignoring data points with RH > 90 %. At RH = 90 %, the uncertainties reported on Fig. 11 are not fully realistic; since the γ parameterization was derived from measurements at RH = 90 %, it seems exaggerated to consider multiplying/dividing factors up to 2 for γ. For both the wet sink and the calculated source at RH < 90 % and for $d_{\mathrm{p}} < 300$ nm, the multipliers never exceed 2 and 0.5. Moreover, we must keep in mind that these uncertainties can be considered as

maximum since extreme multiplying factors were applied on γ values.

The results presented in the previous sections lead to the conclusion that positive small ion properties (size, concentration) are significantly different on event and non-event days but the aerosol ion sink and the ionization rate only show significant differences in summer. At this stage it is thus difficult to link small ion properties to ion sink and production. Thus, in order to investigate the relevance of the positive ionization rate values derived from the balance equation, we compared them with ion production rate estimations from radon measurements. The results related to these estimations are discussed in the following section.

3.3.3 Estimation of the ionization rate based on radon measurements

The main sources for the small ions in the atmosphere are airborne radionuclides (mainly radon, ^{222}Rn) and external radiation (cosmic radiation and gamma radiation from the ground). Since ^{222}Rn is continuously monitored at the Puy de Dôme, it was possible to have an estimation of the contribution of this radionuclide source on the ion production rate. The ionization attributable to the ^{222}Rn was derived from the ^{222}Rn concentration using the decay scheme (three alpha and two beta) and energies from Zhang et al. (2011), assuming that ^{222}Rn was in equilibrium with its short-lived progeny and that 34 eV were needed for the production of one ion pair.

The seasonal variability of ^{222}Rn activity at Puy de Dôme is characterized by lower values during wintertime when air masses are more representative of free tropospheric conditions. In winter, monthly mean ^{222}Rn activity concentrations are lower than $1\,\mathrm{Bq\,m^{-3}}$, while they range from 1 to $2.5\,\mathrm{Bq\,m^{-3}}$ in other seasons. In winter, no significant diurnal cycle of the radon activity is observed whereas during other seasons, the mean diurnal cycle shows an increase between 8:00 and 10:00 UTC, with an average amplitude for the diurnal cycle of $0.43\,\mathrm{Bq\,m^{-3}}$ (Lopez, 2012). This increase corresponds to the rise of the atmospheric boundary layer above the altitude of the station. Similar variability was previously described at the mountain site of Schauinsland (Schmidt et al., 1996).

Concerning the cosmic radiation, there was no measurement available at the Puy de Dôme. Even if cosmic radiation is known to be influenced by solar modulation (with a periodicity of 11 years) and by latitude modulation (Hensen and Van der Hage, 1994), the use of 2 ion pair $\mathrm{cm^{-3}\,s^{-1}}$ as an average value seemed to be applicable at ground level (Hensen and Van der Hage, 1994; Yu, 2002; Usoskin et al., 2004). However, since the pressure at the Puy de Dôme is around 0.86 bar, the value of 2 ion pair $\mathrm{cm^{-3}\,s^{-1}}$ was decreased to 1.7 ion pair $\mathrm{cm^{-3}\,s^{-1}}$.

For gamma radiation, since we had neither measurement nor estimation, we ignored this contribution on a first approximation, assuming it was not driving the daily variation of the total ionization rate. The latter approximation was supported by several studies (Laakso et al., 2004; Hirsikko et al., 2007b; Franchin, 2009) who showed that the contribution of external radiation was certainly important but not responsible for the observed daily variation of the total ionization rate, which was mainly caused by the radon contribution.

Figure 12 shows the ionization rate derived from the balance equation (Q_{calc}) versus the ionization rate obtained from radon measurements and galactic cosmic rays (GCR) estimations (Q_{meas}) as a function of the time of day. On average, the measured and the calculated ionization rates are of the same order of magnitude and display the same temporal variations at the intra-seasonal scale. In winter and spring, the ionization rates derived from the balance equation are slightly smaller than the ionization rates derived from radon measurements, and the difference does not appear to be time dependent. Thus, it seems that in winter and spring, both on event and non-event days, we underestimate the ionization rate when using the balance equation. This could be explained by a misestimated calculated sink. In summer and fall, the ionization rates derived from the balance equation are typically slightly higher than the ionization rates derived from radon measurements. Moreover, the differences between calculated and measured ionization rates spread over a larger range of values compared to winter and spring but they are still not dependent on the time of day.

We must keep in mind that these seasonal differences between measured and calculated ionization rates do not include the gamma radiation contribution and thus might not be quantitatively correct. However, since significant variations in gamma radiation are only seen on the seasonal scale (Hirsikko et al., 2007b; Franchin, 2009), an additional gamma radiation contribution to Q_{meas} would essentially lead to add an almost seasonal constant offset to the difference $Q_{\mathrm{calc}}-Q_{\mathrm{meas}}$. The latter point is further discussed in the following section. It is worth noticing that when considering all the seasons together, both event and non-event days, we obtain $Q_{\mathrm{calc}}-Q_{\mathrm{meas}}$ in the range of $0.19 \pm 2.26\,\mathrm{cm^{-3}\,s^{-1}}$.

Figure 12 suggests that the fraction of the total ionization rate due to radon does not differ between event and non-event days. The confirmation is given by the U test (figure not shown) for all seasons except summer. In summer, the radon contribution appears to be significantly different on event days compared to non-event days from the time period 08:00–18:00 UTC but a closer look at the radon contribution reveals that it is lower on event days. Thus, since radon concentrations are not increased on event days compared to non-event days, it seems that radon is not the determining source for the excess small ions contributing to nucleation on event days.

We have shown so far that positive cluster ions were more numerous on event days compared to non-event days but neither the sources nor the sinks seem to be able to explain these differences. Concerning the source and sink derived from the

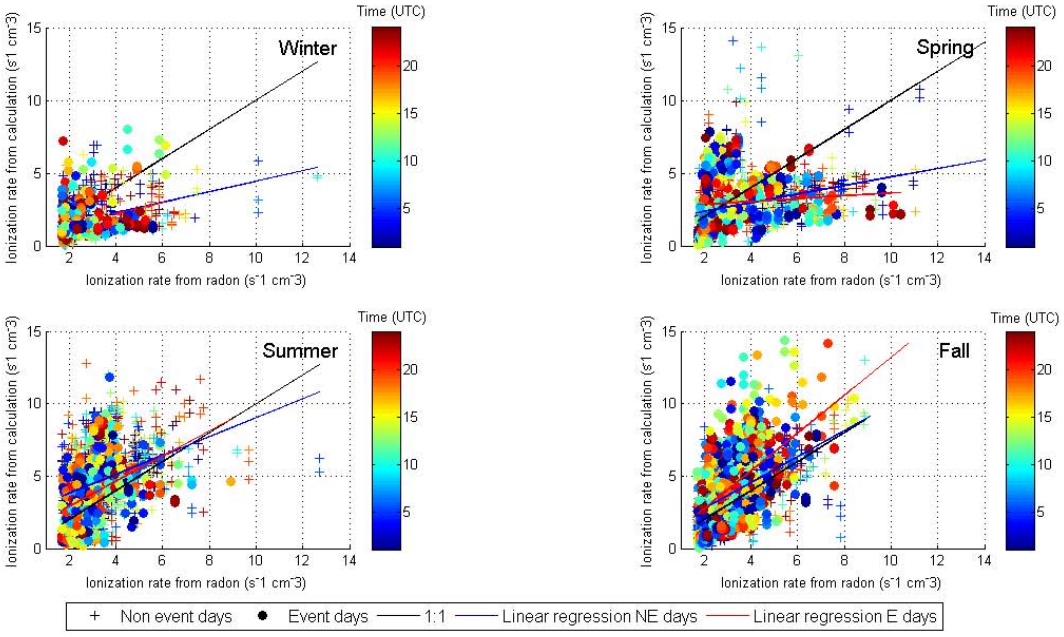

Fig. 12. Positive ionization rate derived from the balance equation versus estimated ionization from radon measured at the Puy de Dôme (February 2007–February 2012) and GCR estimation as a function of time. NPF event days and non-event days are plotted separately (dots and crosses, respectively).

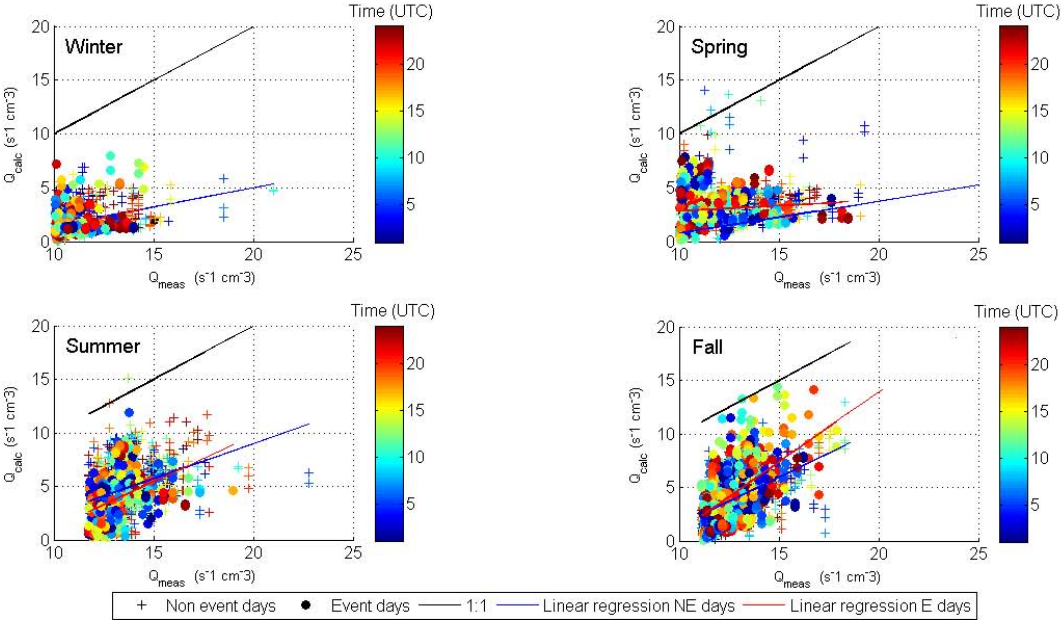

Fig. 13. Positive ionization rate derived from the balance equation versus estimated ionization from radon measured at the Puy de Dôme (February 2007–February 2012) and external radiation contribution (ie., GCR and gamma radiation) as a function of time. NPF event days and non-event days are plotted separately (dots and crosses, respectively).

balance equation, the more plausible explanation comes from an inappropriate use of the equation due to an imbalance between ion sources and sinks which might occur on event days, leading to the fact that the steady state is not verified. When considering measured ionization rates, no more difference can be seen between event and non-event days. Thus it seems that we are missing an additional source for clusters on event days. If gamma radiation shows seasonal variations, we must believe that these variations are not significant enough from one day to another to explain the excess of ions

on event days. The hypothesis of cluster ions formed during nucleation events occurring simultaneously down in the valley and transported to the station also has to be rejected. Indeed, there is no reason for radon not to be transported with clusters. Since we do not detect an increase in the radon concentration on event days, we must believe that the influence of the valley on cluster concentration is low. Thus, the additional source responsible for the excess of ions on event days has not yet been identified.

3.3.4 Sensitivity study on the external radiation contribution to the measured ionization rate

As previously mentioned, there was no measurement of the external radiation contribution to the ionization rate available at the PDD, which lead us, on a first approximation, to neglect the contribution of gamma radiation to the ionization rate. The aim of this section is to further investigate the influence of the gamma radiation contribution on the quantitative estimations of the ionization rate.

For that purpose, we used measurements of the external radiation dose rate (gamma radiation from the soil and GCR) from the Basic Environmental Observatory (BEO) located at peak Moussalain Rila mountain (2925 m a.s.l.), Bulgaria. In their paper, Mishev and Hristova (2011) reported seasonal variations of the dose rate, with higher values in summer and fall. These observations are consistent with other studies concerning BL stations (Hirsikko et al., 2007b; Franchin, 2009). The authors explained the seasonal variations of the dose rate by the increased moisture and the snow cover of the soil during winter and spring, which affect especially gamma radiation from the ground.

We calculated ionization rates from the BEO seasonal average dose rate values by assuming again that 34 eV were needed for the production of one ion pair and air density of $1.29\,\mathrm{kg\,m^{-3}}$. The contribution to the ionization rate from external radiation that we finally obtained was 10.09, 9.74, 11.76 and $11.14\,\mathrm{cm^{-3}\,s^{-1}}$, for winter, spring, summer and fall, respectively. These values are significantly higher than the ionization rates derived from radon measurements only, which display average values in the range 0.94–$1.57\,\mathrm{cm^{-3}\,s^{-1}}$ for the different seasons. These values are quite similar to the ionization rates reported by Franchin (2009) in Hyytiäla: the median total ionization rate over the whole measurement period (March 2000–July 2007) was $10.12\,\mathrm{cm^{-3}\,s^{-1}}$, with a contribution from Rn activity in the range 4–18 %.

If we consider again the difference Q_{calc}–Q_{meas}, with Q_{meas} including now the radon and the external radiation contribution from BEO, we obtain an average value of $-8.90 \pm 2.07\,\mathrm{cm^{-3}\,s^{-1}}$ for all the seasons (Fig. 13). If we assume that Q_{meas} is well estimated, the previous result suggests that we consistently miss a sink in the balance equation, both on event and non-event days. Several studies suggested that dry deposition on vegetation could be part of the missing sink at some stations (e.g. Laakso et al., 2004). However, the forest which surrounds the Puy de Dôme is mainly composed of deciduous trees, which could only justify an additional sink from late spring to mid-fall. No constant sink able to explain the large differences between Q_{calc} and Q_{meas} has yet been identified.

4 Conclusion

We investigated the behaviour of cluster ions (mobility greater than $0.5\,\mathrm{cm^2\,V^{-1}\,s^{-1}}$) in clear sky conditions at the Puy de Dôme station. Concentrations were analysed with respect to the season and to the occurrence of a new particle formation event. We used a data set which spread over five years (February 2007–February 2012), leading to 800 days of measurement.

At the Puy de Dôme, the nucleation frequency was around 24.5 % and displayed an annual variation with three maxima (one in late winter/early spring, one in summer and one in fall). Class II events were found to be dominant in winter and spring (44.7 and 33.1 %, respectively) while "bump-type" events were most significant in summer and fall (65.6 and 40.4 %, respectively).

The monthly medians of the cluster ion concentrations were fluctuating typically between 200 and $600\,\mathrm{cm^{-3}}$ and presented an annual variation with lower values in spring. Positive small ions were less numerous on average than negative ones. The negative cluster ion concentration did not display any diurnal variation whereas on event days, the positive cluster ion concentration exhibited a maximum around noon. Using the Mann–Whitney U test, we showed that during the time period 10:00–16:00 UTC, positive cluster ion concentrations were significantly raised by a factor of 1.12–1.76 during event days compared to non-event days at the same time period. The diameter of the positive cluster ion mode did not show any clear annual variation, with a median typically around 1.2–1.3 nm. On event days, the median diameter of the positive cluster ion mode increased around noon compared to non-event days during all seasons. From the size distribution study, we showed that the diameter increase could not explain the rise of positive ion concentration detected by the AIS, and we concluded that both positive ion size and concentrations were significantly modified on event days during the time period of interest for the nucleation process.

The loss of cluster ions on aerosol particle was found to be predominant compared to the ion recombination, which on average did not exceed 29 % of the total ion sink. The median aerosol ion sink derived from the SMPS size distribution, considering wet aerosol particle diameters, varied in the range of 1.4×10^{-3}–$10.6 \times 10^{-3}\,\mathrm{s^{-1}}$ with the highest values during the warm season due to enhanced dynamics of the BL. The median values of the positive ionization rate derived from the balance equation were in the range

of 1.58 – 3.90 $\mathrm{cm}^{-3}\,\mathrm{s}^{-1}$ with the highest values in summer and fall. The ionization rates derived from the balance equation (Q_{calc}) were compared with a direct estimation of the ion source (Q_{meas}) from ^{222}Rn measurements and a constant GCR contribution of 1.7 ion pair $\mathrm{cm}^{-3}\,\mathrm{s}^{-1}$. For all seasons, Q_{calc} and Q_{meas} were well correlated but Q_{calc} was on average higher in summer and fall. When taking into account seasonal external radiation estimations (GCR and gamma), Q_{meas} always exceeded Q_{calc}. A deeper analysis of the last observation would require a more accurate estimation of the external radiation. This could be obtained from direct measurement of the gamma dose rate at the Puy de Dôme. After a closer analysis of the positive ion sources and sinks, we unexpectedly found that the U test could not clearly distinguish event and non-event days, except in summer. But even in summer, we showed that radon could not explain the excess ions on event days.

Our findings demonstrate that positive cluster ions properties such as the concentration are significantly different on event and non-event days but neither the sinks nor the sources that we considered are able to explain these differences. The excess of small positive ions on event days might be explained by (1) an additional constant source that is missing in our analysis, coupled with the fact that (2) on event days, at least at the beginning of the NPF process, the steady state of the cluster ion concentration is not verified since the production of cluster ions is faster than the loss of these clusters.

Similar analysis of the small cluster concentration and size on event and non-event days should also be done for neutral clusters. This suggestion is supported by the fact that neutral pathways were reported to dominate the formation of neutral clusters (Kulmala et al., 2013).

Appendix A

As previously indicated, the sensitivity study related to the use of the gamma parameterization was done by calculating factors that should multiply the values of the studied parameters when changing the gamma values. The multipliers for the growth factor corresponded to the ratio of the growth factor using parameterized γ to the growth factor obtained after multiplying/dividing parameterized gamma values by 2:

$$\mathrm{GF\_multipliers} = \frac{\mathrm{GF}_{\mathrm{modified}}}{\mathrm{GF}_{\mathrm{initial}}} = \frac{\left(1-\frac{\mathrm{RH}}{100}\right)^{\gamma_{\mathrm{modified}}}}{\left(1-\frac{\mathrm{RH}}{100}\right)^{\gamma_{\mathrm{initial}}}}. \quad \text{(A1)}$$

Then the modified values of the growth factor were used to calculate the aerosol ion sink multipliers:

$$Sa_{\mathrm{wet\_multipliers}} = \frac{Sa_{\mathrm{wet\ modified}}}{Sa_{\mathrm{wet\ initial}}} = \frac{\mathrm{GF}_{\mathrm{modified}}}{\mathrm{GF}_{\mathrm{initial}}} \frac{\int_{d_{\mathrm{p}}} \sqrt{\frac{d_{\mathrm{p}}\cdot\mathrm{GF}_{\mathrm{modified}}-1\,\mathrm{nm}}{d_{\mathrm{p}}\cdot\mathrm{GF}_{\mathrm{modified}}-5\,\mathrm{nm}}} N(d_{\mathrm{p}})dd_{\mathrm{p}}}{\int_{d_{\mathrm{p}}} \sqrt{\frac{d_{\mathrm{p}}\cdot\mathrm{GF}_{\mathrm{initial}}-1\,\mathrm{nm}}{d_{\mathrm{p}}\cdot\mathrm{GF}_{\mathrm{initial}}-5\,\mathrm{nm}}} N(d_{\mathrm{p}})dd_{\mathrm{p}}}. \quad \text{(A2)}$$

The ionization rate multipliers were finally derived from the balance equation, using the modified aerosol ion sink and assuming a constant concentration for positive and negative small ions; this concentration was set to 400 cm^{-3} since it was almost the average annual concentration observed at the Puy de Dôme:

$$Q\_\mathrm{multipliers} = \frac{Q_{\mathrm{modified}}}{Q_{\mathrm{initial}}} = \frac{\alpha\cdot 400^2 + 400\cdot Sa_{\mathrm{wet\ modified}}}{\alpha\cdot 400^2 + 400\cdot Sa_{\mathrm{wet\ initial}}}. \quad \text{(A3)}$$

Acknowledgements. This work was performed within the framework of the Research Infrastructure Action under the FP6 Structuring the European Research Area Program, EUSAAR contract no. RII3-CT-2006-026140, and ACTRIS (Aerosols, Clouds and Trace gases Research Infra Structure Network). It was supported by the LEFE/DFG program within the project "Secondary organic aerosol production in the lower troposphere over western Europe".

Edited by: V.-M. Kerminen

The publication of this article is financed by CNRS-INSU.

References

Asmi, A., Wiedensohler, A., Laj, P., Fjaeraa, A.-M., Sellegri, K., Birmili, W., Weingartner, E., Baltensperger, U., Zdimal, V., Zikova, N., Putaud, J.-P., Marinoni, A., Tunved, P., Hansson, H.-C., Fiebig. M., Kivekäs, N., Lihavainen, H., Asmi, E., Ulevicius, V., Aalto, P.P., Swietlicki, E., Kristensson, A., Mihalopoulos, N., Kalivitis, N., Kalapov, I., Kiss, G., De Leeuw, G., Henzing, B., Harrison, R.M., Beddows, D., O'Dowd, C., Jennings, S.G., Flentje, H., Weinhold, K., Meinhardt, F., Ries, L., and Kulmala, M.: Number size distributions and seasonality of submicron particles in Europe 2008–2009, Atmos. Chem. Phys., 11, 5505–5538, doi:10.5194/acp-11-5505-2011, 2011.

Asmi, E., Sipilä, M., Manninen, H. E., Vanhanen, J., Lehtipalo, K., Gagné, S., Neitola, K., Mirme, A., Mirme, S., Tamm, E., Uin, J., Komsaare, K., Attoui, M., and Kulmala, M.: Results of the first air ion spectrometer calibration and intercomparison workshop, Atmos. Chem. Phys., 9, 141–154, doi:10.5194/acp-9-141-2009, 2009.

Biraud, S., Ciais, P., Ramonet, M., Simmonds, P., Kazan, V., Monfray, P., O'Doherty, S., Spain, T. G., and Jennings, S. G.: European greenhouse gas emissions estimated from continuous atmospheric measurements and radon 222 at Mace Head, Ireland, J. Geophys. Res., 105, 1351–1366, doi:10.1029/1999JD900821, 2000.

Boulon, J., Sellegri, K., Venzac, H., Picard, D., Weingartner, E., Wehrle, G., Collaud Coen, M., Bütikofer, R., Flückiger, E., Baltensperger, U., and Laj, P.: New particle formation and ultrafine charged aerosol climatology at a high altitude site in the Alps (Jungfraujoch, 3580 m a.s.l., Switzerland), Atmos. Chem. Phys., 10, 9333–9349, doi:10.5194/acp-10-9333-2010, 2010.

Boulon, J., Sellegri, K., Hervo, M., Picard, D., Pichon, J.-M., Fréville, P. and Laj, P.: Investigation of nucleation events vertical extent: a long term study at two different altitude sites, Atmos. Chem. Phys., 11, 5625–5639, doi:10.5194/acp-11-5625-2011, 2011.

Chalmers, J. A.: Atmospheric electricity, Pergamon Press, Oxford, London, UK, 1967.

Dal Maso, M., Kulmala, M., Riipinen, I., Wagner, R., Hussein, T., Aalto, P. P. and Lehtinen, K. E.: Formation and growth of fresh atmospheric aerosols: eight years of aerosol size distribution data from SMEAR II, Hyytiala, Finland, Boreal Environ. Res., 10, 323–336, 2005.

Dhanorkar, S. and Kamra, A. K.: Diurnal variation of ionization rate close to ground, J. Geophys. Res. Atmos., 99, 18523–18526, doi:10.1029/94JD01335, 1994.

Dickinson, R. E.: Solar variability and the lower atmosphere, B. Am. Meteorol. Soc., 56, 1240–1248, 1975.

Duplissy, J., Gysel, M., Sjogren, S., Meyer, N., Good, N., Kammermann, L., Michaud, V., Weigel, R., Martins dos Santos, S., Gruening, C., Villani, P., Laj, P., Sellegri, K., Metzger, A., McFiggans, G.B., Wehrle, G., Richter, R., Dommen, J., Ristovski, Z., Baltensperger, U., and Weingartner, E.: Intercomparison study of six HTDMAs: results and recommendations, Atmos. Meas. Tech., 2, 363–378, doi:10.5194/amt-2-363-2009, 2009.

Enghoff, M. B. and Svensmark, H.: The role of atmospheric ions in aerosol nucleation – a review, Atmos. Chem. Phys., 8, 4911–4923, doi:10.5194/acp-8-4911-2008, 2008.

Franchin, A.: Relation between ^{222}Rn concentration and ion production rate in boreal forest, in: Proceedings of the Finish center of Excellence and Graduate School in "Physics, Chemistry, Biology and Meteorology of Atmospheric composition and Climate Change" Annual Workshop 27–29 April 2009, edited by: M. Kulmala, J. Bäck, and T. Nieminen, Rep. Ser. Aerosol Sci., 102, 105–108, 2009.

Freney, E. J., Sellegri, K., Canonaco, F., Boulon, J., Hervo, M., Weigel, R., Pichon, J. M., Colomb, A., Prévôt, A. S. H., and Laj, P.: Seasonal variations in aerosol particle composition at the puy-de-Dôme research station in France, Atmos. Chem. Phys., 11, 13047–13059, doi:10.5194/acp-11-13047-2011, 2011.

Hämeri, K., Väkevä, M., Aalto, P. P., Kulmala, M., Swietlicki, E., Zhou, J., Seidl, W., Becker, E., and O'dowd, C. D.: Hygroscopic and CCN properties of aerosol particles in boreal forests, Tellus B, 53, 359–379, 2001.

Hensen, A. and Van der Hage, J. C. H.: Parameterization of cosmic radiation at sea level, J. Geophys. Res., 99, 10693–10695, doi:10.1029/93JD01226, 1994.

Hirsikko, A., Laakso, L., Horrak, U., Aalto, P. P., Kerminen, V., and Kulmala, M.: Annual and size dependent variation of growth rates and ion concentrations in boreal forest, Boreal Environ. Res., 10, 357–369, 2005.

Hirsikko, A., Bergman, T., Laakso, L., Dal Maso, M., Riipinen, I., Hõrrak, U. and Kulmala, M.: Identification and classification of the formation of intermediate ions measured in boreal forest, Atmos. Chem. Phys., 7, 201–210, doi:10.5194/acp-7-201-2007, 2007a.

Hirsikko, A., Paatero, J., Hatakka, J., and Kulmala, M.: The 222Rn activity concentration, external radiation dose and air ion production rates in a boreal forest in Finland between March 2000 and June 2006, Boreal Environ. Res., 12, 265–278, 2007b.

Hirsikko, A., Nieminen, T., Gagné, S., Lehtipalo, K., Manninen, H. E., Ehn, M., Hõrrak, U., Kerminen, V.-M., Laakso, L., McMurry, P. H., Mirme, A., Mirme, S., Petäjä, T., Tammet, H., Vakkari, V., Vana, M., and Kulmala, M.: Atmospheric ions and nucleation: a review of observations, Atmos. Chem. Phys., 11, 767–798, doi:10.5194/acp-11-767-2011, 2011.

Hoppel, W. A., Anderson, R. V., and Willett, J. C.: Atmospheric electricity in the planetary boundary layer, The Earth's Electrical Environment, National Academy Press, Washington, DC, USA, 149–165, 1986.

Hõrrak, U., Salm, J., and Tammet, H.: Diurnal variation in the concentration of air ions of different mobility classes in a rural area, J. Geophys. Res., 108, 4653, doi:10.1029/2002JD00240, 2003.

Hõrrak, U., Aalto, P. P., Salm, J., Komsaare, K., Tammet, H., Mäkelä, J. M., Laakso, L., and Kulmala, M.: Variation and balance of positive air ion concentrations in a boreal forest, Atmos. Chem. Phys., 8, 655–675, doi:10.5194/acp-8-655-2008, 2008.

IPCC: IPCC(AR4):Climate change 2007: Impacts, Adaptation and Vulnerability. Contribution of working group II to the Fourth Assessment Report of the Intergovernmental Panel on Climate Change, edited by: Parry, M. L., Canziani, O. F., Palutikof, J. P., van der Linden, P. J., and Hanson, C. E., Cambridge University Press, Cambridge,, 2007.

Israël, H.: Atmospheric Electricity: Fundamentals, conductivity, ions, Israel Program for Scientific Translations, Jerusalem, 1970.

Kangasluoma, J., Junninen, H., Lehtipalo, K., Mikkilä, J., Vanhanen, J., Attoui, M., Sipilä, M., Worsnop, D., Kulmala, M., and Petäjä, T.: Remarks on Ion Generation for CPC Detection Efficiency Studies in Sub-3-nm Size Range, Aerosol Sci. Technol., 47, 556–563, doi:10.1080/02786826.2013.773393, 2013.

Kazil, J., Harrison, R. G., and Lovejoy, E. R.: Tropospheric New Particle Formation and the Role of Ions, Space Sci. Rev., 137, 241–255, doi:10.1007/s11214-008-9388-2, 2008.

Kerminen, V.-M., Paramonov, M., Anttila, T., Riipinen, I., Fountoukis, C., Korhonen, H., Asmi, E., Laakso, L., Lihavainen, H., Swietlicki, E., Svenningsson, B., Asmi, A., Pandis, S. N., Kulmala, M., and Petäjä, T..: Cloud condensation nuclei production associated with atmospheric nucleation: a synthesis based on existing literature and new results, Atmos. Chem. Phys., 12, 12037–12059, doi:10.5194/acp-12-12037-2012, 2012.

Kim, C. S., Okuyama, K., and De la Mora, J. F.: Performance evaluation of an improved particle size magnifier (PSM) for single nanoparticle detection, Aerosol Sci. Technol., 37, 791–803, 2003.

Komppula, M., Vana, M., Kerminen, V. M., Lihavainen, H., Viisanen, Y., Horrak, U., Komsaare, K., Tamm, E., Hirsikko, A., and

Laakso, L.: Size distributions of atmospheric ions in the Baltic Sea region, Boreal Environ. Res., 12, 323–336, 2007.

Kuang, C., Chen, M., McMurry, P. H., and Wang, J.: Modification of Laminar Flow Ultrafine Condensation Particle Counters for the Enhanced Detection of 1 nm Condensation Nuclei, Aerosol Sci. Technol., 46, 309–315, 2012.

Kulmala, M. and Kerminen, V.-M.: On the formation and growth of atmospheric nanoparticles, Atmos. Res., 90, 132–150, doi:10.1016/j.atmosres.2008.01.005, 2008.

Kulmala, M., Vehkamäki, H., Petäjä, T., Dal Maso, M., Lauri, A., Kerminen, V.-M., Birmili, W., and McMurry, P. H.: Formation and growth rates of ultrafine atmospheric particles: a review of observations, J. Aerosol Sci., 35, 143–176, 2004.

Kulmala, M., Kontkanen, J., Junninen, H., Lehtipalo, K., Manninen, H. E., Nieminen, T., Petäjä, T., Sipilä, M., Schobesberger, S., Rantala, P., Franchin, A., Jokinen, T., Järvinen, E., Aijälä, M., Kangasluoma, J., Hakala, J., Aalto, P. P., Paasonen, P., Mikkilä, J., Vanhanen, J., Aalto, J., Hakola, H., Makkonen, U., Ruuskanen, T., Mauldin, R. L., Duplissy, J., Vehkamäki, H., Bäck, J., Kortelainen, A., Riipinen, I., Kurtén, T., Johnston, M. V., Smith, James N., Ehn, M., Mentel, T. F., Lehtinen, K. E. J., Laaksonen, A., Kerminen, V.-M., and Worsnop, D. R.: Direct Observations of Atmospheric Aerosol Nucleation, Science, 339, 943–946, doi:10.1126/science.1227385, 2013.

Laakso, L., Mäkelä, J. M., Pirjola, L., and Kulmala, M.: Model studies on ion-induced nucleation in the atmosphere, J. Geophys. Res., 107, AAC5–1–AAC5–19, doi:10.1029/2002JD002140, 2002.

Laakso, L., Petäjä, T., Lehtinen, K. E. J., Kulmala, M., Paatero, J., Hõrrak, U., Tammet, H., and Joutsensaari, J.: Ion production rate in a boreal forest based on ion, particle and radiation measurements, Atmos. Chem. Phys., 4, 1933–1943, doi:10.5194/acp-4-1933-2004, 2004.

Laakso, L., Gagné, S., Petäjä, T., Hirsikko, A., Aalto, P. P., Kulmala, M., and Kerminen, V.-M.: Detecting charging state of ultrafine particles: instrumental development and ambient measurements, Atmos. Chem. Phys., 7, 1333–1345, doi:10.5194/acp-7-1333-2007, 2007.

Lihavainen, H., Komppula, M., Kerminen, V.-M., Järvinen, H., Viisanen, Y., Lehtinen, K., Vana, M., and Kulmala, M.: Size distributions of atmospheric ions inside clouds and in cloud-free air at a remote continental site, Boreal Environ. Res., 12, 337–344, 2007.

Lopez, M.: Estimation des émissions de gaz à effet de serre à différentes échelles en France à l'aide d'observations de haute précision, Université Paris Sud-Paris XI, Paris, France, 2012.

Lovejoy, E. R., Curtius, J., and Froyd, K. D.: Atmospheric ion-induced nucleation of sulfuric acid and water, J. Geophys. Res., 109, D08204, doi:10.1029/2003JD004460, 2004.

Luts, A., Parts, T.-E., and Vana, M.: New aerosol particle formation via certain ion driven processes, Atmos. Res., 82, 547–553, doi:10.1016/j.atmosres.2006.02.011, 2006.

Mäkelä, J. M., Riihelä, M., Ukkonen, A., Jokinen, V., and Keskinen, J.: Comparison of mobility equivalent diameter with Kelvin-Thomson diameter using ion mobility data, J. Chem. Phys., 105, 1562–1571, doi:doi:10.1063/1.472017, 1996.

Makkonen, R., Asmi, A., Kerminen, V.-M., Boy, M., Arneth, A., Hari, P., and Kulmala, M.: Air pollution control and decreasing new particle formation lead to strong climate warming, Atmos. Chem. Phys., 12, 1515–1524, doi:10.5194/acp-12-1515-2012, 2012.

Manninen, H. E., Petäjä, T., Asmi, E., Riipinen, I., Nieminen, T., Mikkilä, J., Horrak, U., Mirme, A., Mirme, S., and Laakso, L.: Long-term field measurements of charged and neutral clusters using Neutral cluster and Air Ion Spectrometer (NAIS), Boreal Environ. Res, 14, 591–605, 2009.

Manninen, H. E., Franchin, A., Schobesberger, S., Hirsikko, A., Hakala, J., Skromulis, A., Kangasluoma, J., Ehn, M., Junninen, H., Mirme, A., Mirme, S., Sipilä, M., Petäjä, T., Worsnop, D. R., and Kulmala, M.: Characterisation of corona-generated ions used in a Neutral cluster and Air Ion Spectrometer (NAIS), Atmos. Meas. Tech., 4, 2767–2776, doi:10.5194/amt-4-2767-2011, 2011.

Mirme, A., Tamm, E., Mordas, G., Vana, M., Uin, J., Mirme, S., Bernotas, T., Laakso, L., Hirsikko, A. and Kulmala, M.: A wide-range multi-channel Air Ion Spectrometer, Boreal Environ. Res., 12, 247–264, 2007.

Mirme, S. and Mirme, A.: The mathematical principles and design of the NAIS – a spectrometer for the measurement of cluster ion and nanometer aerosol size distributions, Atmos. Meas. Tech., 6, 1061–1071, doi:10.5194/amt-6-1061-2013, 2013.

Mishev, A. and Hristova, E.: Gamma Background Measurements at BEO Moussala, Institute for Nuclear Research and Nuclear Energy, Bulg. Acad. Sci., 1–18, 2011.

Nieminen, T., Paasonen, P., Manninen, H. E., Sellegri, K., Kerminen, V.-M., and Kulmala, M.: Parameterization of ion-induced nucleation rates based on ambient observations, Atmos. Chem. Phys., 11, 3393–3402, doi:10.5194/acp-11-3393-2011, 2011.

Polian, G., Lambert, G., Ardouin, B., and Jegou, A.: Long-range transport of continental radon in subantarctic and antarctic areas, Tellus B, 38B, 178–189, doi:10.1111/j.1600-0889.1986.tb00185.x, 1986.

Rosen, J. M., Hofmann, D. J., and Gringel, W.: Measurements of ion mobility to 30 km, J. Geophys. Res., 90, 5876–5884, doi:10.1029/JD090iD04p05876, 1985.

Schmidt, M.: Measurement and balancing of anthropogenic greenhouse gases in Germany, University of Heidelberg, Heidelberg, Germany, 1999.

Schmidt, M., Graul, R., Sartorius, H., and Levin, I.: Carbon dioxide and methane in continental Europe: a climatology, and ^{222}Radon-based emission estimates, Tellus B, 48, 457–473, 1996.

Schobesberger, S., Franchin, A., Vana, M., and Kulmala, M.: Analysis of the ionization rate at a boreal forest measurement site in Finland in 2008, in: Proceedings of the Finish center of Excellence and Graduate School in "Physics, Chemistry, Biology and Meteorology of Atmospheric composition and Climate Change" Annual Workshop 27–29 April 2009, edited by: Kulmala, M., Bäck, J., and Nieminen, T., Report series in Aerosol Sciences 102, 386–389, 2009.

Seaton, A., Godden, D., MacNee, W., and Donaldson, K.: Particulate air pollution and acute health effects, The Lancet, 345, 176–178, doi:10.1016/S0140-6736(95)90173-6, 1995.

Sloan, T. and Wolfendale, A. W.: Testing the proposed causal link between cosmic rays and cloud cover, Environ. Res. Lett., 3, 024001, doi:10.1088/1748-9326/3/2/024001, 2008.

Tammet, H.: Aerosol electrical density: Interpretation and principles of measurement, Report Series in Aerosol Science (Helsinki), 19, 128–133, 1991.

Tammet, H., Hõrrak, U., Laakso, L., and Kulmala, M.: Factors of air ion balance in a coniferous forest according to measurements in Hyytiälä, Finland, Atmos. Chem. Phys., 6, 3377–3390, doi:10.5194/acp-6-3377-2006, 2006.

Usoskin, I. G., Gladysheva, O. G., and Kovaltsov, G. A.: Cosmic ray-induced ionization in the atmosphere: spatial and temporal changes, J. Atmos. Sol.-Terr. Phys., 66, 1791–1796, 2004.

Vana, M., Hirsikko, A., Tammet, E., Aalto, P., Kulmala, M., Verheggen, B., Cozic, J., Weingartner, E. and Baltensperger, U.: Characteristics of air ions and aerosol articlesat the high alpine research station Jungfraujoch, Proceedings of 7-th International Aerosol Conference, the American Association for Aerosol Research (AAAR), ISBN978-0-9788735-0-9, 1427, 2006.

Vana, M., Ehn, M., Petäjä, T., Vuollekoski, H., Aalto, P., De Leeuw, G., Ceburnis, D., O'Dowd, C. D., and Kulmala, M.: Characteristic features of air ions at Mace Head on the west coast of Ireland, Atmos. Res., 90, 278–286, 2008.

Vanhanen, J., Mikkilä, J., Lehtipalo, K., Sipilä, M., Manninen, H. E., Siivola, E., Petäjä, T. ,and Kulmala, M.: Particle size magnifier for nano-CN detection, Aerosol Sci. Technol., 45, 533–542, 2011.

Venzac, H., Sellegri, K., and Laj, P.: Nucleation events detected at the high altitude site of the Puy de Dôme Research Station, France, Boreal Environ. Res., 12, 345–359, 2007.

Venzac, H., Sellegri, K., Villani, P., Picard, D., and Laj, P.: Seasonal variation of aerosol size distributions in the free troposphere and residual layer at the puy de Dôme station, France, Atmos. Chem. Phys., 9, 1465–1478, doi:10.5194/acp-9-1465-2009, 2009.

Wilhelm, S., Eichkorn, S., Wiedner, D., Pirjola, L., and Arnold, F.: Ion-induced aerosol formation: new insights from laboratory measurements of mixed cluster ions HSO_4-(H_2SO_4)a(H_2O)w and H+(H_2SO_4)a(H_2O)w, Atmos. Environ., 38, 1735–1744, 2004.

Yli-Juuti, T., Riipinen, I., Aalto, P. P., Nieminen, T., Maenhaut, W., Janssens, I. A., Claeys, M., Salma, I., Ocskay, R., and Hoffer, A.: Characteristics of new particle formation events and cluster ions at K-puszta, Hungary, Boreal Environ. Res., 14, 683–698, 2009.

Yu, F.: Altitude variations of cosmic ray induced production of aerosols: Implications for global cloudiness and climate, J. Geophys. Res., 107, 1118, doi:10.1029/2001JA000248, 2002.

Zhang, K., Feichter, J., Kazil, J., Wan, H., Zhuo, W., Griffiths, A. D., Sartorius, H., Zahorowski, W., Ramonet, M., Schmidt, M., Yver, C., Neubert, R. E. M., and Brunke, E.-G.: Radon activity in the lower troposphere and its impact on ionization rate: a global estimate using different radon emissions, Atmos. Chem. Phys., 11, 7817–7838, doi:10.5194/acp-11-7817-2011, 2011.

Zhou, J., Swietlicki, E., Berg, O. H., Aalto, P. P., Hameri, K., Nilsson, E. D., and Leck, C.: Hygroscopic properties of aerosol particles over the central Arctic Ocean during summer, J. Geophys. Res., 106, 32111–32123, 2001.